IZMIR DEMOCRACY UNIVERSITY

NATURAL & APPLIED SCIENCES JOURNAL

IDUNAS

E-ISSN: 2645-9000

Year: 2021

Volume: 4, Issue: 1

Table of Contents

Sayfa

1. Research Article 1
   a. Elemental Concentration and Physicochemical Properties of Soils under Different Landuses in Gashua a Sahel Region of Nigeria 1
   b. Domestic Software Developed for Updating of Finite Element Models and Experimental Modal Analysis of Structures 15
   c. Experimental Modal Analysis and Structural Health Monitoring of the Double Curvature Deriner Arch Dam 22
   d. An Image Segmentation Method for Wound Healing Assay Images 30
   e. Microbial Activities and Physicochemical Properties of Pesticide Treated Soils and Waters 38

DOI: 10.38061/idunas.815402

IDUNAS	NATURAL & APPLIED SCIENCES JOURNAL	2021 Vol. 4 No. 1 (1-14)

Elemental Concentration and Physicochemical Properties of Soils under Different Landuses in Gashua a Sahel Region of Nigeria

Research Article

Busari, K. A.[1*], Alhassan, I.[2*], Onuk, O. G.[1*]

[1]Department of Physics, Federal University Gashua, Yobe State, Nigeria

[2] Department of Agronomy, Federal University Gashua, Yobe State, Nigeria

Author E-mails
ialhassand@gmail.com
*Correspondance to: Alhassan, I., Department of Agronomy, Federal University Gashua, Yobe State, Nigeria.
DOI: 10.38061/idunas.815402

Received: 23.10.2020; Accepted: 25.01.2021

Abstract

Soil elements assessment under various land uses is vital in knowing the status of the soils in terms of fertility and toxicity. Therefore, a study was conducted to investigate some elements concentrations of soils under three different land uses in Gashua, Yobe State, Nigeria. Samples were randomly taken at 0-15 and 15-30 cm soil depth intervals from land uses. The land uses are Dry upland (DU), Lowland (LL) and Residential area (RA). The selected elements were determined in the laboratory using Atomic Absorption Spectrophotometer (AAS), while some physicochemical properties were determined using routine soil analysis methods. The results indicated significantly higher concentrations of Iron (6.96 mg kg^{-1}), Manganese (3.12 mg kg^{-1}) and clay content (12.88%), except for Nickel which was higher in DU (2.36 mg kg^{-1}) but at par with the content in LL (2.04 mg kg^{-1}) land use. There was no significant difference within the following soil elements within the study location: Cadmium (Cd), Chromium (Cr), Copper (Cu) and Lead (Pb) were below detection limit within the soils of the chosen land use types. Generally the soils textural class is sandy loam with higher mean bulk density (1.62g cm^{-3}) and a neutral soil pH (6.81). The physicochemical properties and elements investigated didn't show significant differences with soil depth. The basic elemental concentrations within the soils were mostly adequate for crop production, except Zn, with little variability within the landuse. They were generally below the utmost ecological risk permissible level set by WHO and FAO.
Keywords: Gashua, land use, soil texture, trace elements.

1. INTRODUCTION

Soil as a non-renewable resource and dynamic nature is prone to rapid degradation with land misuse (Eswaran et al., 2001). Land use is defined as the type of activities to which land is subjected to, including the inputs added, manipulation and management practices employed to produce, utilize and preserve (Ufot et al., 2016). Judicious land use is a principal factor underlying sustained agricultural production, maintenance and enhancement of the productive potential and life-support processes of natural resources

(Srivastava et al., 1993). Different land uses, because of the different activities taking place on them may impact the soils physico-chemical properties differently, which may also require different management strategies. The physical properties of soils determine their adaptability to cultivation and the level of chemical and biological activity in the soil. Soil physical properties affect to a large extent soil water content and air for proper growth of plants. Soil physical properties can also be affected greatly by changes in land use systems and management practices (Tilahun, 2007; Sanchez, 1976).

Properties such as soil texture, structure, bulk density, porosity, moisture content and retention capacity are among the common soil physical properties. Soil texture refers to the relative percentage of sand, silt and clay within a soil layer and Bulk density is an indicator of soil compaction and reflects the soil ability to function for structural support, water and solute movement, and soil aeration (Arshad et al., 1996). Soil texture is an important aspect because it affects other physical and chemical properties such as water holding capacity and base saturation. It is also the primary factor determining the vertical distribution pattern and storage of carbon, nitrogen and phosphorus in savanna soils (Tabor et al., 2017). Bulk density is another physical property of soil that has a great influence on the soil porosity and compaction. It may cause restrictions to root growth and poor movement of air and water through the soil (Weil and Brady, 2017).

Elements are released overtime due transformations and various reactions of some minerals in the soil inherited from the parent materials. These elements perform different functions, some are essential in plant and animal nutrition, while others, their roles are not link to nutrition and their presence above known safe limits may endanger the environment as well as both plant and animal health (Weil and Brady, 2017). Elements like Cobalt (Co) Copper (Cu), Iron (Fe), Manganese (Mn), Nickel (Ni) and Zinc (Zn) are considered essential in plant and animal nutrition while, Cadmium (Cd), Chromium (Cr) and Lead (Pb) are not considered essential in their nutrition (Weil and Brady, 2017).

Timely and periodic assessment of the impact of land uses on elemental availability, distribution and ecological risks is indispensible for sustainable management of the soils of any area. The study is exploratory due to lack of information on background concentrations of the elements in soils of the study area. The objective of the study is to evaluate the concentrations of Cd, Co, Cr, Cu, Fe, Mn, Ni, Pb and Zn in soils within three land use types in Gashua, Yobe State, Nigeria.

2. MATERIALS & METHODS

Description of the Study Area

The study was conducted at Gashua in Bade Local Government Area of Yobe State, Northeast Nigeria. It is situated 190 km North West of Damaturu, the State Capital. It is located between longitudes 9° 00’ and 10° 30’ N and latitudes 9° 30’ and 10° 30’E and at an altitude of 293 meters above sea level. The area is situated in the Sahel savanna agro-climatic zone with a unimodal rainfall pattern of an average annual rainfall of 300 - 430 mm and maximum rain is received between August and September. The annual mean minimum and mean maximum temperatures at the study area are 12 and 44°C respectively.

Land Use Types

Three land use types’ namely dry upland arable farms (arable crops such as millet, cowpea, sesame, sorghum etc. are grown), lowland farms along the floodplains of river Yobe (vegetables, rice and wheat are the common crops cultivated in these areas) and residential area (inhabited by human settlements) were studied in Gashua in Bade Local Government Area of Yobe State, Nigeria.

Soil Sample Collection

Stratified random-composite sampling design was adopted for the survey. Three representative soil samples were collected randomly using a soil auger from each of the four replicate of each land use type at two soil depths of 0 – 15cm and 15 – 30cm. The samples per replicate per depth were composite for laboratory analysis. Sampling cylinders were also used in taking undisturbed samples from each replicate closer to auger sampling points for bulk density determination (Estefan et al., 2013). The augured soil samples were then air-dried at room temperature for 5 days, sieved before analysis.

Soil Analysis

The soil properties analyzed include soil particle size distribution (PSD), bulk density (BD), pH, Cobalt (Co), Cadmium (Cd), Chromium (Cr), Copper (Cu), Iron (Fe), Manganese (Mn), Nickel (Ni), Lead (Pb) and Zinc (Zn). Soil particle size distribution was determined by the hydrometric method (Estefan et al., 2013). Soil bulk density was determined by the undisturbed soil core sampling method. The soil samples were dried in an oven at 104^{o}C to constant weights and calculated as:

$$\text{BD (g cm}^{-3}) = \frac{W}{V} \quad (1)$$

Where: W = weight of oven dry soil (g) and V = volume of soil sample (cm^{-3}). The pH of the soils was measured in a 1:2 (soil: water) suspension potentiometrically using digital pH meter (Estefan et al., 2013).

Soil samples were digested using Nitric-sulphuric-perchloric acid digestion method as modified from Idera et al (2015). Five gram of soil samples were measured into 125ml Beaker and a mixture of 2ml, 4ml and 25ml, of concentrated H_2SO_4, $HClO_4$ and HNO_3 were added respectively for digestion on a hot plate in a fumes hood. The digested sample was allowed to cool at room temperature and 50ml of deionized water was added and then filtered through a 0.45µ Millipore membrane filter paper. The filtered samples were then made up to 100ml with deionized water. The concentration of the selected elements (Cd, Co, Cr, Cu, Fe, Mn, Ni, Pb and Zn) were then determined from the extract with Atomic Absorption Spectrophotometer (PerkinElmer 900T Boston, USA) using appropriate lamp.

Statistical Analysis

The analyzed data from the laboratory tests were subjected to descriptive statistics and analysis of variance technique using R version 3.6.1 statistical package. Differences among the means were separated using HSD criterion at 5% significance level (R, 2019)

3. RESULTS & DISCUSSION

The summary statistics of the soil properties determined were presented in Table 1. The results indicated normally distribution for the variables tested except for clay (1.47) and Mn (1.82) which were positively skewed. The means of the soil properties were not far from their median values; this indicated existence of very few outliers or none. The Coefficient of variation of the soil properties were low for soil pH (6.76%), BD (7.85%), sand (8.63%), Fe (9.03%), Zn (11.37%); moderate for Silt (28.80%) and higher in clay (38.56%), Co (48.66%), Mn (66.70%) and Ni (77.15%) according to the ratings in Tabi and Ogunkunle (2007). This revealed considerable variability as such site-specific management may be required.

Table-1. Descriptive Statistics of the Mean values of the Physico-chemical Properties and Elemental Concentrations in the Soils of the Study Areas

Variables	Min	Max	Mean	Median	IQR	SD	SEM	CV (%)	Skewness
Sand (%)	61.00	88.00	76.00	76.00	8.50	6.56	1.34	8.63	-0.24
Silt (%)	7.00	21.00	14.00	14.00	6.50	4.03	0.82	28.80	0.08
Clay (%)	4.00	23.00	10.00	9.50	4.00	3.86	0.79	38.56	1.47
BD (g cm^{-3})	1.38	1.85	1.62	1.66	0.12	0.13	0.03	7.85	-0.57
pH	6.13	7.86	6.81	7.73	0.63	0.46	0.09	6.76	0.66
Co (mg kg^{-1})	0.01	0.38	0.20	0.22	0.14	0.10	0.02	48.66	-0.16
Mn (mg kg^{-1})	0.48	5.46	1.89	1.72	0.98	1.26	0.26	66.70	1.82
Ni (mg kg^{-1})	0.06	4.59	1.74	2.10	2.18	1.34	0.27	77.15	0.39
Fe (mg kg^{-1})	5.79	7.89	6.69	6.57	0.81	0.60	0.12	9.03	0.42
Zn (mg kg^{-1})	0.68	1.22	0.95	0.97	0.10	0.11	0.02	11.37	-0.18
Cd	ND	ND	ND	ND					
Cr	ND	ND	ND	ND					
Cu	ND	ND	ND	ND					
Pb	ND	ND	ND	ND					

Min = minimum, Max = maximum, IQR = interquartile range, SD = standard deviation, SEM = standard error of the mean, CV = coefficient of variation.

The soil particle size distribution (PSD) showed that the sand and silt fractions did not significantly differ among land use types (Figure 1 and 2 respectively). The overall mean of the clay fraction was found to be significantly higher in the Lowland (12.88%) compared to Dry upland (8.61%) and Residential area (8.50%) (Figure 3). High clay content in Lowland may presumably be due to the physiographic location of Lowland and the nature of the erosional sediments deposited and intensive soil management practices that promote further weathering processes could be a possible reason for higher clay content (Negasa et al., 2017). The dominant soil textural class (Sandy loam) throughout the study area indicates the homogeneity of soil forming processes and the similarity of parent materials. Soil bulk density was also not significantly affected by land use effects (Figure 4). The highest (1.67 g cm^{-3}) mean value of soil bulk density was recorded under cultivated lowland area (LL) and the lowest (1.57 g cm^{-3}) mean BD was found in Dry Upland (DU). Similar mean bulk density value (1.63 g cm^{-3}) was also reported for soils of Bade LGA in Yobe State, Nigeria by Alhassan et al. (2018). The average bulk densities recorded in the study area are marginally high for crop growth, because it was reported that for optimum movement of air and water through the soil, it is generally desirable for the soil to have a BD of < 1.5gcm^{-3} and that in general bulk densities greater than 1.6gcm^{-3} tend to restrict root growth (Hunt and Gilkes, 1992; McKenzie et al., 2004). The high bulk density recorded could be attributed to the high sand content of the soils as was reported that sand content have a greater effect on bulk density than other soil properties (Chaudhari et al., 2013). This was further substantiated by Lal (2006) who reported that normal range of bulk densities for clay is 0.90 to 1.40 gcm-3 and a normal range for sand is 1.40 to 1.90 gcm-3 with potential root restriction occurring at ≥ 1.40 gcm-3 for clay and ≥ 1.60 gcm-3 for sand.

Soil pH showed little variability across the land uses with a mean value of 6.81 and ranged from 6.57 to 6.95 (Figure 5), the soils are then categorized as neutral (6.51 to 7.5) by Weil and Brady (2017). Soil pH is an important secondary determinant of nutrients availability and transport as it affects their water solubility in the soil. The pH values of 6.5 to 7.5 is considered ideal for crop production (Estefan et al., 2013) therefore, the soil pH values of the study area is considered good for crop production and will not require any amendment.

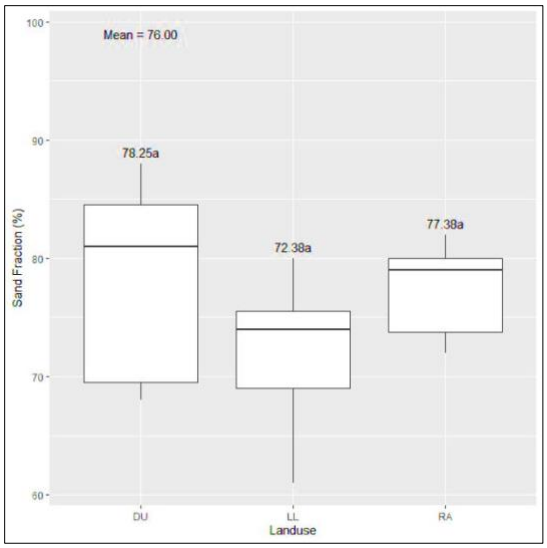

Figure-1. Sand Fraction Distribution of the Soils Under Landuse types (Dry Upland Farm (DU), Lowland Farm (LL) and Residential Area (RA)

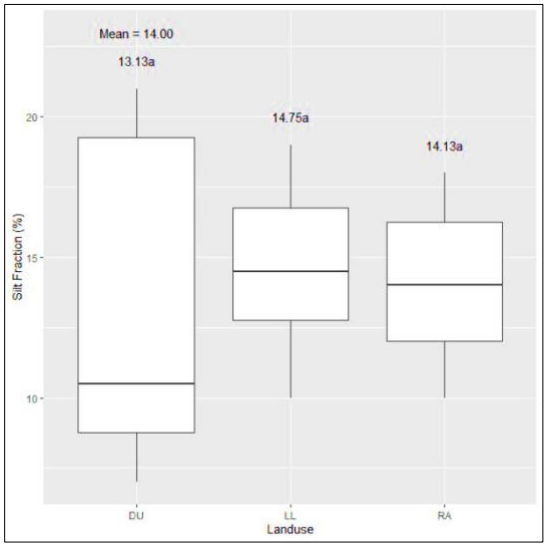

Figure-2. Silt Fraction Distribution of the Soils under Landuse types (Dry Upland Farm (DU), Lowland Farm (LL) and Residential Area (RA)

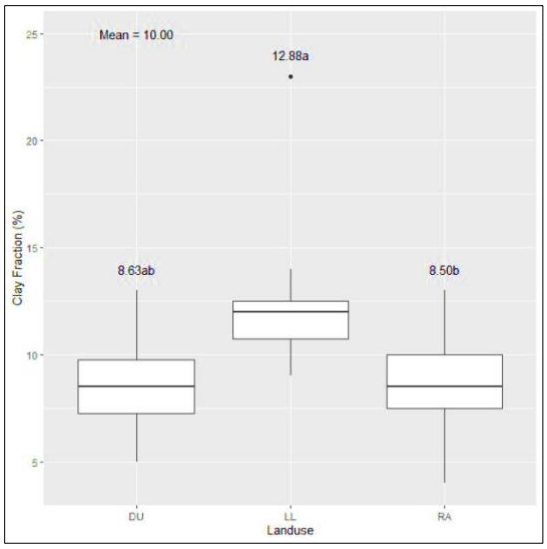

Figure-3. Clay Fraction Distribution of the Soils under Landuse types (Dry Upland Farm (DU), Lowland Farm (LL) and Residential Area (RA)

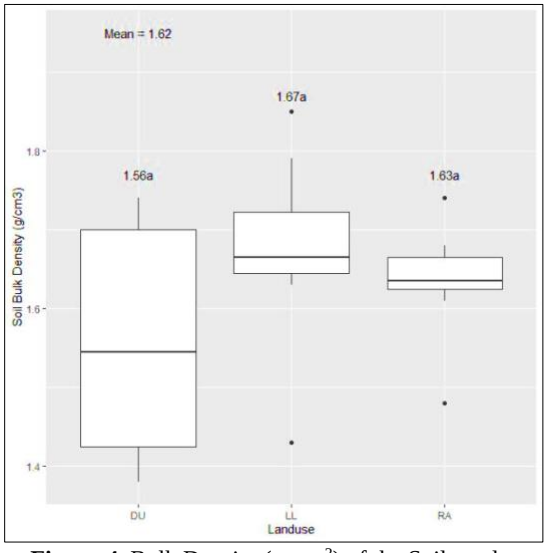

Figure-4. Bulk Density (g cm^{-3}) of the Soils under Landuse types (Dry Upland Farm (DU), Lowland Farm (LL) and Residential Area (RA)

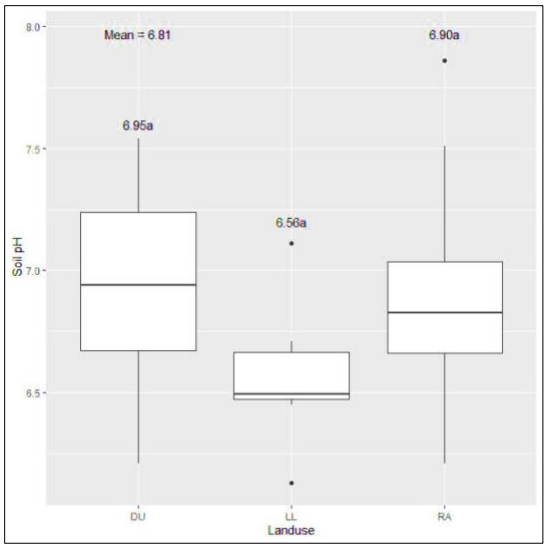

Figure-5. pH of the Soils under Landuse types (Dry Upland Farm (DU), Lowland Farm (LL) and Residential Area (RA))

The mean elemental concentrations ($mgkg^{-1}$) in the soils of the land use types were presented in Figures 6 to 10. Result showed that Cobalt (Co) was not significantly different between the land uses (Figure 6). Cobalt is considered an essential nutrient in trace amounts for ruminant animals, largely due its requirement for rumen bacteria, atmospheric N_2-fixation by microorganisms and for plants (Ma and Hooda, 2010). A concentration of Co (4.6–9.1 $mgkg^{-1}$) was reported for some soils in Nigeria (Agbenin et al., 2009). The mean concentration of Co recorded at the study sites were below the WHO/FAO (2001) ecological risk permissible limit of 100 $mgkg^{-1}$ for soils.

The mean concentration of iron (Fe) ranged from 6.23 to 6.96 $mgkg^{-1}$ with a mean value of 6.69 $mgkg^{-1}$ (Table 1). The result indicated significant difference between the land uses with high concentration in LL which was at par with RA and lower in DU (Figure 7). The mean concentration of Fe recorded was above the critical limit (>5 $mgkg^{-1}$) for crop production (Esu, 1991) and below the FEPA (1991) guidelines for heavy metals in soils ecological risk threshold value of 400.00 $mgkg^{-1}$. In agreement to our findings Mulima et al. (2015) reported higher values of Fe for the soils of similar agro-ecological zone and Munkholm et al. (1993) reported that Fe and Mn deficiencies in tropical Africa are rare. The high mean Fe content in the soil indicates that Fe deficiency is not likely for crops grown on these soils. However, the presence of Fe in high concentrations in soils could lead to the formation of phlintite upon complex chemical reactions Plinthosols are more common type of soils in the wetter parts of the Sahel and are always rich in iron (Decker's et al, 1995).

Significantly higher Mn concentration (3.12 mg kg^{-1}) was recorded in LL and lower at DU (1.12 mg kg^{-1}) at par with RA (1.41 mg kg^{-1}) (Figure 8). The mean value (1.88 mg kg^{-1}) indicated moderate availability for crop production (Esu, 1991; Shukla and Gupta, 1975). It was further supported by Horneck et al. (2011) that soil test values for Mn of between 1 and 5 ppm are usually sufficient for crop production. In contrast Mulima et al. (2015) reported a very high mean value of Mn (10.23 $mgkg^{-1}$) for the soils of similar environment in Nigeria.

Although the concentration of Iron and Manganese recorded are adequate for crop production, the values are far below those reported in other parts of Nigeria. 10.8 mg kg^{-1} and 34 mg kg^{-1} respectively for Fe and Mn were reported for soils of Northern Guinea Savanna region of Nigeria by Mustapha et al. (2011), 19.6 mg kg^{-1} for Fe in Sudan Savanna by Oyinlola and Chude (2010), 22.5 mg kg^{-1} and 21.5 mg $kg^{-1}$for soils of Bauchi, northern guinea Savanna (Oluwadare et al., 2013) and 14.48 mg kg^{-1} and 17.59 mg $kg^{-1}$for soils of Billiri, northern guinea Savanna of Nigeria (Ibrahim et al., 2011). This could be attributed to the neutral pH in where the availability of Fe and Mn tend to be low. It was reported that with increase in soil

pH decreases the solubility of most trace elements, which often leads to their low concentrations in soil solution (Kabata-Pendias, 2011).

Nickel is an essential micro nutrient for plants and is equally important to animals. As with other trace metals, elevated Ni concentrations in soils have potential negative impact on plants, microorganisms and animals (Ma and Hooda, 2010). The mean concentrations of nickel recorded in the soil samples ranged from 0.80 to 2.36 $mgkg^{-1}$ with a mean value of 1.73 $mgkg^{-1}$ (Figure 9). This value is lower than 12.6–25.7 mg kg^{-1} reported for some soils in northern Nigeria (Agbenin et al., 2009) and Ogundele et al. (2015) reported 1.83 – 14.87 $mgkg^{-1}$ as the mean concentration of Ni in soil for North Central Nigeria. The mean concentrations of Ni recorded from the studied land uses were below the WHO/FAO (2001) permissible limit of 50 $mgkg^{-1}$ for soils. Large variability of Ni could be attributed to spatial variability in the sampling points within the lowland area as reported that micronutrient content in the soil often shows considerable spatial variation (Hengl et al., 2017), while the low mean value may be due to high pH level of the soils. The Ni concentration in soils of the studied area may not pose environmental problem and is above lowest required level (< 0.5 $mgkg^{-1}$) for plant nutrition (Guodong et al, 2020).

The mean concentration of zinc (Zn) ranged from 0.90 to 0.98 $mgkg^{-1}$ with a mean value of 0.95 $mgkg^{-1}$ (Figure 10). This is in agreement with Mulima et al. (2015) who reported low mean Zn status (0.85 $mgkg^{-1}$) for the soils of Geidam in Yobe State, Nigeria and lower than the mean value of 3.00 $mgkg^{-1}$ recorded for Kano urban agricultural lands in Nigeria (Dawaki et al., 2013) and 31.17 $mgkg^{-1}$ for some soils in South Western Nigeria (Adagunodo et al., 2018). Zinc deficiency was also reported that it predominates the list of micronutrients that are deficient in sub Saharan African arable soils (Kihara et al., 2020), therefore crops like rice and maize that are susceptible to Zn deficiency may require Zn fertilization in the study area. The mean concentration of Zn recorded in the study area was below the WHO/FAO (2001) ecological risk permissible limit of 300 $mgkg^{-1}$ for soils.

Cadmium (Cd), Chromium (Cr), Copper (Cu) and Lead (Pb) were not detected in the soils of the study area as such they pose no threat to the environment (Table 1).

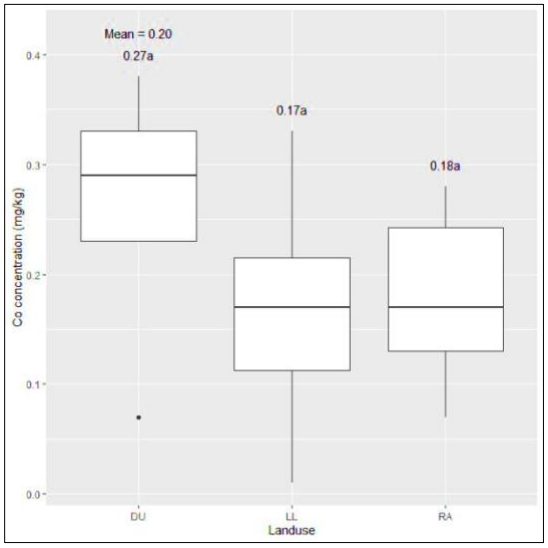

Figure-6. Cobalt (Co) concentration (mg kg^{-1}) of the Soils under Landuse types (Dry Upland Farm (DU), Lowland Farm (LL) and Residential Area (RA))

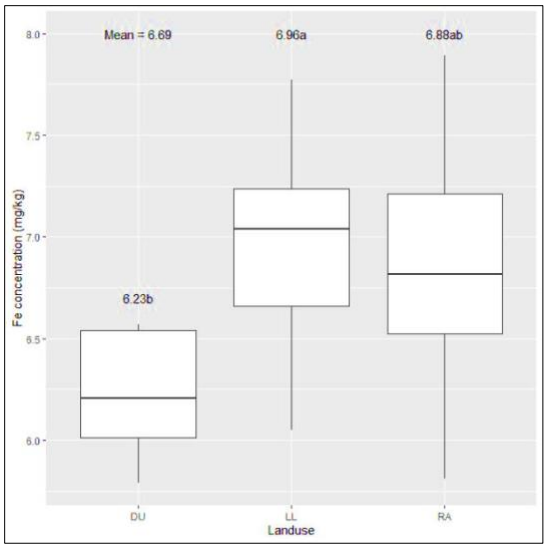

Figure-7. Iron (Fe) concentration (mg kg^{-1}) of the Soils under Landuse types (Dry Upland Farm (DU), Lowland Farm (LL) and Residential Area (RA))

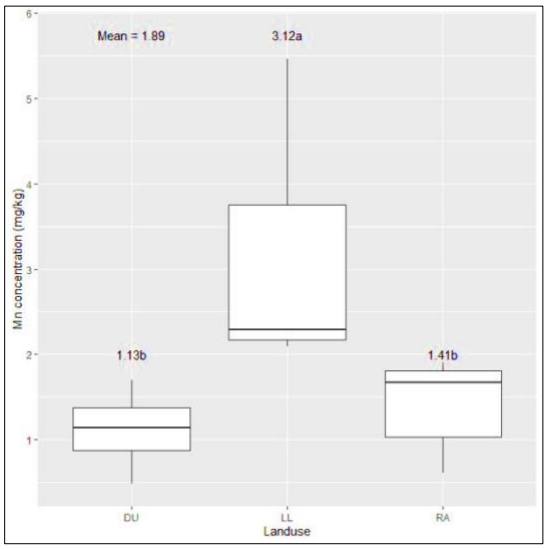

Figure-8. Manganese (Mn) concentration (mg kg^{-1}) of the Soils under Landuse types (Dry Upland Farm (DU), Lowland Farm (LL) and Residential Area (RA))

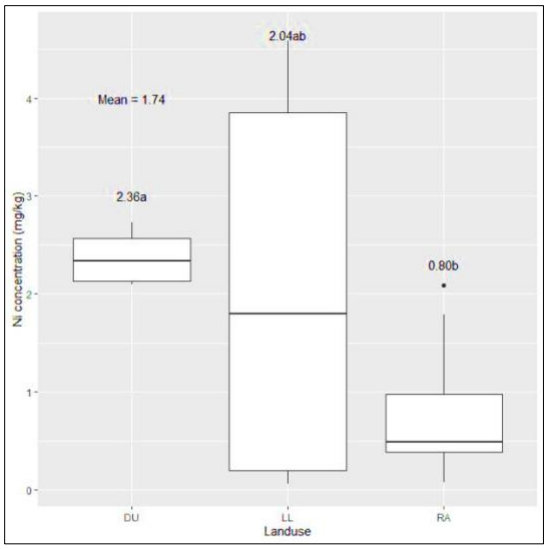

Figure-9. Nickel (Ni) concentration (mg kg^{-1}) of the Soils under Landuse types (Dry Upland Farm (DU), Lowland Farm (LL) and Residential Area (RA))

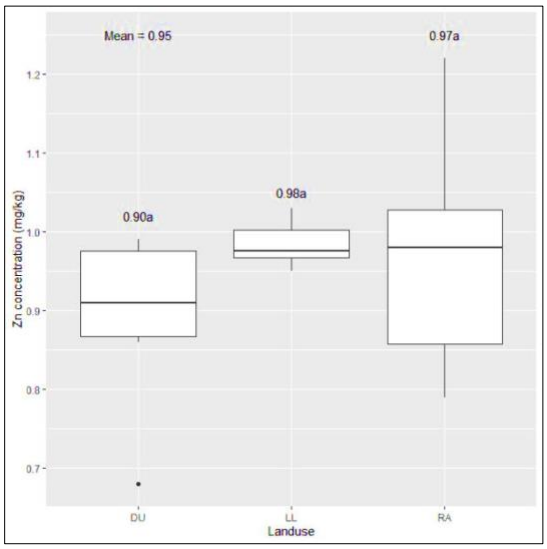

Figure-10. Zinc (Zn) concentration (mg kg^{-1}) of the Soils under Landuse types (Dry Upland Farm (DU), Lowland Farm (LL) and Residential Area (RA))

The soil depth (0-15 and 15-30cm) was found not to have significant influence on all the measured soil variables (Table 2), but clay fraction showed high coefficient variability (37.50%) and in the concentrations elements such as Co (48.94), Mg (40.76%), Mn (67.95%) and Ni (78.87%).

Table-2. Effect of Soil Depth on the Soil Properties

Soil Properties	0 - 15cm	15 -30cm	Mean	SE	CV (%)
Sand (%)	74.5	77.5	76	2.66	8.58
Silt (%)	14.33	13.67	14	1.68	29.35
Clay (%)	11.17	8.83	10	1.53	37.5
Textural class	SL	SL			
Bulk Density (g cm^{-3})	1.58	1.66	1.62	0.05	7.6
pH	6.76	6.85	6.81	0.19	6.87
Calcium ($mgkg^{-1}$)	2.91	3.23	3.07	0.23	18.32
Cadmium ($mgkg^{-1}$)	ND	ND	ND		
Cobalt ($mgkg^{-1}$)	0.19	0.22	0.20	0.04	48.94
Chromium ($mgkg^{-1}$)	ND	ND	ND		
Copper ($mgkg^{-1}$)	ND	ND	ND		
Potassium ($mgkg^{-1}$)	0.52	0.51	0.51	0.01	6.61
Iron ($mgkg^{-1}$)	6.92	6.46	6.69	0.23	8.53
Magnesium ($mgkg^{-1}$)	2.85	3.48	3.17	0.53	40.76
Nickel ($mgkg^{-1}$)	1.71	1.76	1.73	0.56	78.87
Lead ($mgkg^{-1}$)	ND	ND	ND		
Zinc ($mgkg^{-1}$)	0.98	0.92	0.95	0.04	11.03

LL = lowland, RA = residential area, DU = dry upland, SE = standard error, CV = coefficient of variation, ND = not detected

4. CONCLUSION

The results showed that five of the elements analyzed (Co, Fe, Mn, Ni and Zn) were present in soil samples at the three landuses sites, while Cu, Cr, Cd, and Pb were not detected. Significant differences were found between the land uses in the concentrations of Fe, Mn and Ni, higher values were recorded under LL except for Ni while lower concentrations were mostly recorded in DU. Generally, the concentrations of the elements in soils under varying landuses studied are within the required concentrations for crop production except for Zn. The elemental concentrations in the soils do not exceed the maximum permissible concentration limit according to USEPA (2002) and WHO/FAO (2001) guidelines.

There is a need for regular assessment and monitoring of these elements in the study area in order to sustain agricultural production and protect the environment as well as human and animal health from the hazards that elevated levels of the elements may pose. The variability of the concentrations under difference landuses may require site specific management. Addition of organic matter (OM) can be useful in improving soil physical condition, reduce compaction, supply plant nutrients and maintain elemental balance in the soil.

5. ACKNOWLEDGEMENT

Authors acknowledged the TETFUND Nigeria through Federal University, Gashua, Nigeria for providing the financial support to carry out the above research.

6. CONFLICTS OF INTEREST

The authors declare no conflict of interest.

7. REFERENCES

1. Adagunodo, L.A., Sunmonu, T.A. and Emetere, M.E. (2018). Heavy metals' data in soils for agricultural activities. Data in Brief, 18: 1847-1855. https://doi.org/10.1016/j.dib.2018.04.115

2. Agbenin, J.O., Danko, M. and Welp, G. (2009). Soil and vegetable compositional relationships of eight potentially toxic metals in urban garden fields

from northern Nigeria. J. Sci. Food Agric., 89: 49-54. doi:10.1002/jsfa.3409

3. Alhassan, I., Gashua, A.G., Dogo, S., Sani, M. (2018). Physical properties and organic matter content of the soils of Bade in Yobe State, Nigeria. Int. J. Agric. Environ. Food Sci., 2(4), 160-163. DOI: 10.31015/jaefs.18027

4. Arshad, M. A., Lowery, B. & Grossman, B. (1996). Physical Tests for Monitoring Soil Quality. In: Doran, J. W., Jones, A. J. (Eds.). Methods for assessing soil quality. Madison, WI

5. Bhatt, R. (2019). Importance of Soil Texture. (retrieved from https://www.scribd.com on 30 December, 2019)

6. Chaudhari, P.R., Ahire, D.V., Ahire, V.D., Chkravarty, M. and Maity, S. (2013). Soil Bulk Density as related to Soil Texture, Organic Matter Content and available total Nutrients of Coimbatore Soil. International Journal of Scientific and Research Publications, 3(2):1-8

7. Dawaki, U.M., Dikko, A.U., Noma, S.S. and Aliyu, U. (2013). Heavy Metals and Physicochemical Properties of Soils in Kano Urban Agricultural Lands. Nigerian Journal of Basic and Applied Science, 21(3): 239-246. Doi.org/10.4314/inbas.v21i3.9

8. Deckers, J., Dondeyne, S., Vandekerckhoven, L. and Raes, D. (1995). Major soils and their formation in the West African Sahel. In: Meizan, K.M., C.M.S. Wopereis, M. Dungkuhn, J. Decker's & T.R. Randokph (Eds). Irrigated rice in Sahel: prospects for sustainable development. West African Rice Development Association, WARDA/ADRAO, Saint Louis, Senegal, 23-35.

9. Estefan, G., Sommer, R. and Ryan, J. (2013). *Methods of Soil, Plant and Water Analysis*: A manual for the West Asia and North Africa region, 3rd ed. ICARDA, Beirut, Lebanon. P 243

10. Eswaran, H., Lal, R. and Reich, P.F. (2001). Land degradation: an overview. In: Bridges EM, Hannam ID, Oldeman LR et al.(eds) Responses to land degradation. Proc. 2nd. International Conference on land degradation and desertification, Khon Kaen, Thailand. Oxford, New Delhi

11. Federal Environmental Protection Agency [FEPA](1991). National Guidance and Standards for Industrial Effluents, Gaseous Emissions and Hazardous Waste Management in Nigeria. Federal Government, Nigeria.

12. Guodong L., Simonne, E. H. and Yuncong, L. (2020). Nickel Nutrition in Plants. UF/IFAS Extension series of the Horticultural Sciences Department, no.HS1191. Available at https://edis.ifas.ufl.edu.

13. Hengl, T., Leenaars, J. G., Shepherd, K. D., Walsh, M. G., Heuvelink, G. B., Mamo, T., et al. (2017). Soil nutrient maps of Sub-Saharan Africa: Assessment of soil nutrient content at 250 m spatial resolution using machine learning. NutrientNutrient Cycling in Agroecosystems, 109(1), 77–102.

14. Horneck, D.A., Sullivan, D.M., Owen, J.S. and Hart, J.M. (2011). *Soil Test Interpretation Guide.* EC 1478. Corvallis, OR: Oregon State University Extension Service

15. Hunt, N. and Gilkes, R. (1992). *Farm Monitoring Handbook*. The University of Western Australia: Nedlands, WA.

16. Ibrahim A.K., Usman A., Abubakar, B. and Aminu, U.H. (2011). Extractable micronutrients status in relation to other soil properties in Billiri Local Government Area, Gombe State, *Journal of Soil Science and Environmental Management.* 3(10):282–285.

17. Idera, F., Omotola, O., Adedayo, A. and Paul, U. J. (2015). Comparison of Acid Mixtures Using Conventional Wet Digestion Methods for Determination of Heavy Metals in Fish. Journal of Scientific Research & Reports. 8(7): 1-9. DOI: 10.9734/JSRR/2015/19717

18. Kabata-Pendias, A. (2011). *Trace Elements in Soils and Plants*, CRC Press, Boca Raton, Florida, USA.

19. Kihara, J., Bolo, P., Kinyua, M., Rurinda, J. and Piikki, K. (2020). Micronutrient deficiencies in African soils and the human nutritional nexus: opportunities with staple crops. Environ Geochem Health (2020) 42:3015–3033. https://doi.org/10.1007/s10653-019-00499-w.

20. Lal, R. (2006). *Encyclopedia of Soil Science*. Taylor and Francis, Florida, USA.

21. Ma, Y. and Hooda, P. S. (2010). Chromium, Nickel and Cobalt In: P. S. Hooda (Ed.). *Trace Elements in Soils*. John Wiley & Sons Ltd, United Kingdom. pp596

22. McKenzie, N.J., Jacquier, D.J., Isbell, R.F. and Brown, K.L. (2004). *Australian Soils and Landscapes*: An Illustrated Compendium. CSIRO Publishing: Collingwood, Victoria.

23. Mulima I. M., Ismaila M. Shafiu, M. I. and Benisheikh, K. M. (2015). Status and Distribution of Some Available Micronutrients in Sudan and Sahel Savanna Agro-Ecological Zones of Yobe State, Nigeria. Journal of Environmental Issues and Agriculture in Developing Countries, 7(1):18-29

24. Munkholm, L.J., Esu, I. and Moberg, J.P. (1993). Trace elements in some northern Nigerian soils. *Commun. Soil Sci. Plant* Anal. 24:657–672.

25. Mustapha, S., Voncir, N., Umar, S. and Abdulhamid, N. S. (2011). Status and Distribution of some Available Micronutrients in *Haplic usterts* of Akko Local Government Area, Gombe State, Nigeria. *International Journal of Soil Science*, 6(4):267-274

26. Negasa, T., Ketema, H., Legesse, A., Sisay, M., & Temesgen, H. (2017). Variation in soil properties under different land use types managed by small-holder farmers along the toposequence in southern Ethiopia. Geoderma, 290, 40–50.

27. Ogundele, D.T., Adio, A.S. and Oludele, O.E. (2015). Heavy Metal Concentrations in Plants and Soil along Heavy Traffic Roads in North Central Nigeria. *Journal of Environmental and Analytical Toxicology*. **5(6)**:1-5. Doi.10.4172/2161-0525.1000334

28. Oluwadare, D.A., Voncir, N., Mustapha, S. and Mohammed, G.U. (2013). Evaluation and Enhancement of Available Micronutrients Status of Cultivated Soil of Nigeria Guinea Savanna Using Organic and Inorganic Amendments. *IOSR Journal of Agriculture and Veterinary Science,* **3(5)**:62-68.

29. Oyinlola, E.Y. and Chude, V.O. (2010). Status of available nutrients of the basement complex rock–derived alfisols in northern Nigeria savanna. *Tropical and Subtropical Agroecosystems*, 12(2):229-237.

30. R Core Team (2019). R: A language and environment for statistical computing. R Foundation for Statistical Computing, Vienna, Austria. URL https://www.R-project.org/.

31. Shukla, U. C. and Gupta, B. L. (1975). "Response of Mn application and evaluation of chemical extractants to determine available Mn in some arid brown soils of Haryana", *Journal of the Indian Society of Soil Science,* 23(3):357-364

32. Srivastava, j. P., Tamboli, P. M., English, J. C., Lal, R. and Stewart, B. A. (1993). Conserving Soil Moisture and Fertility in the Warm Seasonally Dry Tropics. World Bank Technical Paper number 221

33. Tabi, F.O. and Ogunkunle, A.O. (2007). Spatial variation of some soil physico-chemical properties of an Alfisol in southwestern Nigeria. *Nigerian Journal of Soil and Environmental Resources*, 7:82-91.

34. Tabor, N. J., Myers, T. S. & Michel, L.A. (2017). Sedimentologist's Guide for Recognition, Description, and Classification of Paleosols.

35. Tilahun, G. (2007). Soil Fertility Status as Influenced by different Land Uses in Maybar Areas of South Wello Zone, North Ethiopia. Master of Science in Agriculture (Soil Science) Thesis Haramaya University, Ethiopia.

36. Ufot, U.O., Iren, O.B. and Chikere Njoku, C.U. (2016). Effects of land use on soil physical and chemical properties in Akokwa area of Imo State, Nigeria. International Journal of Life Sciences Scientific Research 2(3): 273-278.

37. US Environmental Protection Agency [USEPA] (2002). Supplemental guidance for developing soil screening levels for superfund sites. Office of Solid Waste and Emergency Response, Washington, D.C. http://www.epa.gov/superfund/health/conmedia/soil/index.htm

38. Weil, R. R. and Brady, N. C. (2017). *Nature and Properties of Soils,* 15th edition. Pearson Education, Inc. Delhi, India.

39. WHO/FAO. (2001). Codex alimentarius commission. Food additives and contaminants. Joint FAO/WHO Food Standards Programme, ALINORM 10/12A. Retrieved on 6 September 2020 from www.transpaktrading.com/static/pdf/research/achemistry/introTofertilizers.pdf

DOI: 10.38061/idunas.851721

IDUNAS	NATURAL & APPLIED SCIENCES JOURNAL	2021 Vol. 4 No. 1 (15-21)

Domestic Software Developed for Updating of Finite Element Models and Experimental Modal Analysis of Structures

Research Article

Ahmet Can Altunışık[1*], Fatih Yesevi Okur[1*]

[1]Department of Civil Engineering, Karadeniz Technical University, Trabzon, Turkey.

Author E-mails:
ahmetcan@ktu.edu.tr
yesevi@ktu.edu.tr
*Correspondance to: Ahmet Can Altunışık, Department of Civil Engineering, Karadeniz Technical University, Trabzon, Turkey.
DOI: 10.38061/idunas.851721

Received: 01.01.2021; Accepted:01.03.2021

Abstract

Reinforced concrete structures used in many areas of our daily life constitute an important part of the building stock in the construction sector. There are many buildings such as reinforced concrete buildings, bridges, tunnels, mosques and dams, and the construction of new buildings in line with the need continues. Many uncertainty factors play a role in the design phase of these structures from the dimensioning as a result of the analysis performed under the required loadings to the implementation phase in the field. Many unpredictable factors such as errors in the analysis, defects in materials and workmanship affect the success rate of the project of the structure. For this purpose, Experimental Modal Analysis method, which is widely used in the literature, is used to determine the success rate of new structures, to determine the dynamic characteristics and damage conditions of existing structures and structural health monitoring. Natural frequencies, which are the dynamic variables of the structure obtained by experimental modal analysis techniques, and mode shapes and damping ratios corresponding to these frequencies are used in the examination of the current state and structural properties of the structures. However, this experimental data can be obtained by with foreign-source software by allocating large budgets. The results of the native experimental modal analysis and finite element model update software developed within the scope of doctoral thesis are compared with the results of the existing software in the literature. As the application, raw signal data of Gülburnu Bridge and scaled Type-1 Arch Dam constructed in laboratory environment were used. The experimental results of the developed software and the existing software were found to be closely related to each other.

Keywords: Dynamic characteristics, Experimental modal analysis, Structural health monitoring.

1. INTRODUCTION

Experimental Modal Analysis method is used to determine the dynamic characteristics of the structures depending on experimental measurement methods. In this method, vibration signals from accelerometers placed on the structure are collected and dynamic characteristics are obtained from raw

vibration data processed using up-to-date software. The determination of dynamic characteristics using analytical and experimental methods brings along the need to compare the results obtained and to interpret the differences between the results. Generally, the differences that may occur are due to uncertain parameters (material and section properties, boundary conditions) taken into account during analytical analysis based on finite element model. If the difference between analytical and experimental dynamic characteristics is around 5-10%, it is accepted that the analytical dynamic characteristics reflect the current state of the structure. However, if this value is greater than 5-10%, it is accepted that the analytical dynamic characteristics do not reflect the current state of the building. In this case, the finite element model of the structure should be improved according to the experimental measurement data [1-5]. Thus, the differences between the results are minimized and a finite element model reflecting the current state of the building is obtained.

Damage detection methods are generally based on the change of dynamic characteristics such as frequency, mode shape and damping ratio. Structures can be damaged over time for various reasons. For this reason, the structural conditions of engineering structures should be monitored periodically or continuously by experimental methods and the damage conditions should be determined early. Thus, future destructions can be prevented.

Within the scope of this study, the results of domestic software developed in order to obtain dynamic characteristics by processing experimental data (Dynamic Modal) and to detect damage by updating finite element models (Dynamic Update) were verified by comparing them with the literature.

2. DYNAMIC MODAL

With the Dynamic Modal software, dynamic characteristics are obtained from the experimental raw signals of the structures. Enhanced Frequency Domain Decomposition (EFDD) and Stochastic Subspace Identification (SSI) methods are used in signal processing. In EFDD Method, Fast Fourier Transform, Power Spectrum, Cross-Power Spectrum, Singular Value Decomposition methods are used. In SSI Method, the processes of creating past / future signals with the help of Hankel Matrix of signals in time environment, obtaining system matrices and determining the stability diagram are performed. Figure 1 presents some views of the Dynamic Modal software. As an example, the dynamic characteristics of the bridge were determined using raw signal data of Gülburnu Highway Bridge. Figure 2 presents some views of the Gülburnu Highway Bridge. The graphs of the results of the Dynamic Modal and Operational Modal Analysis [6] software are given in Figure 3.

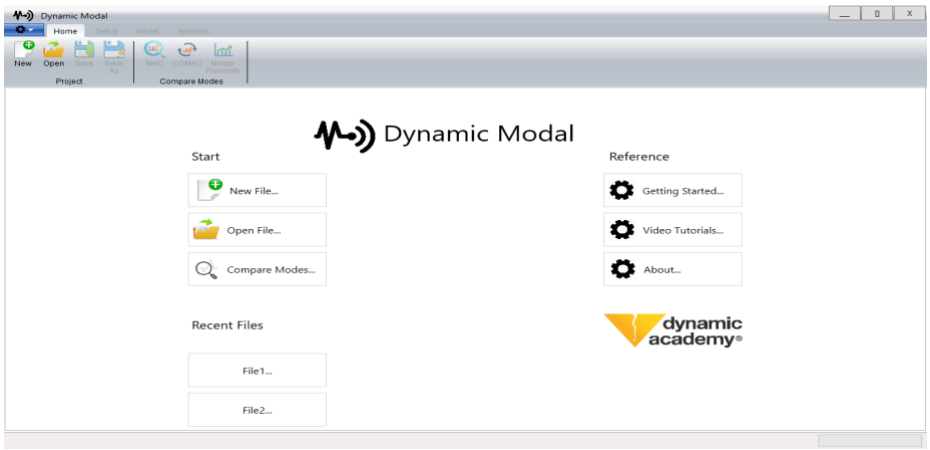

a) Login menu of Dynamic Modal software

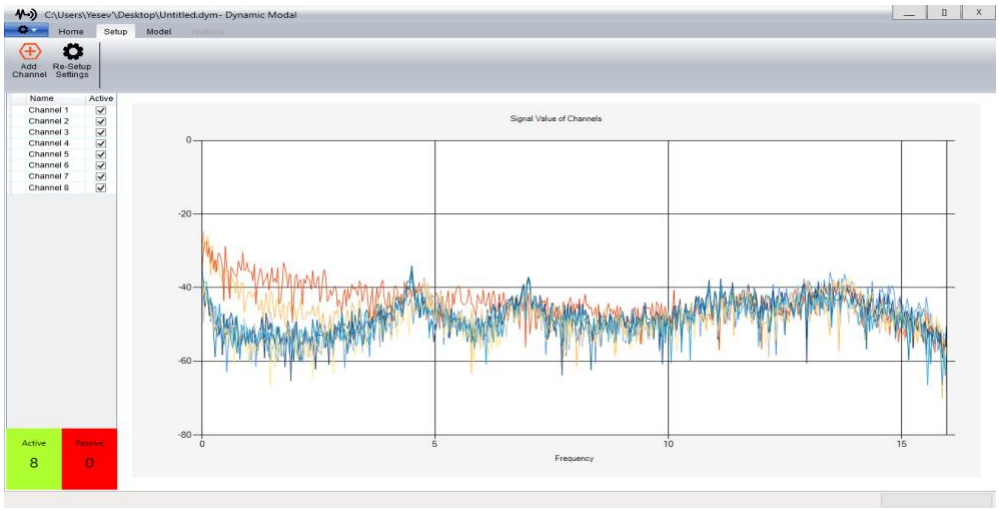

b) Transfer of raw signals to software

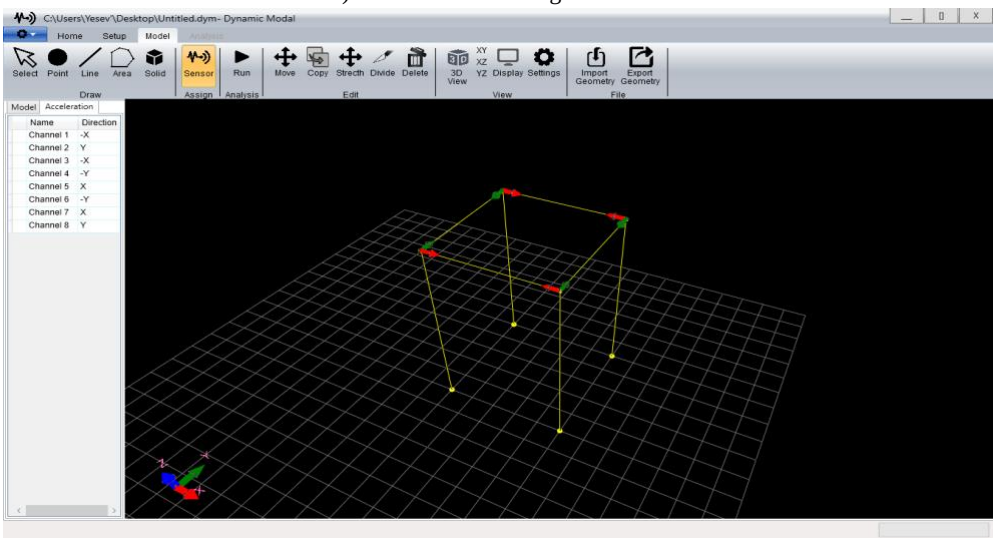

c) Creating the model geometry

Figure 1. Some images of Dynamic Modal software.

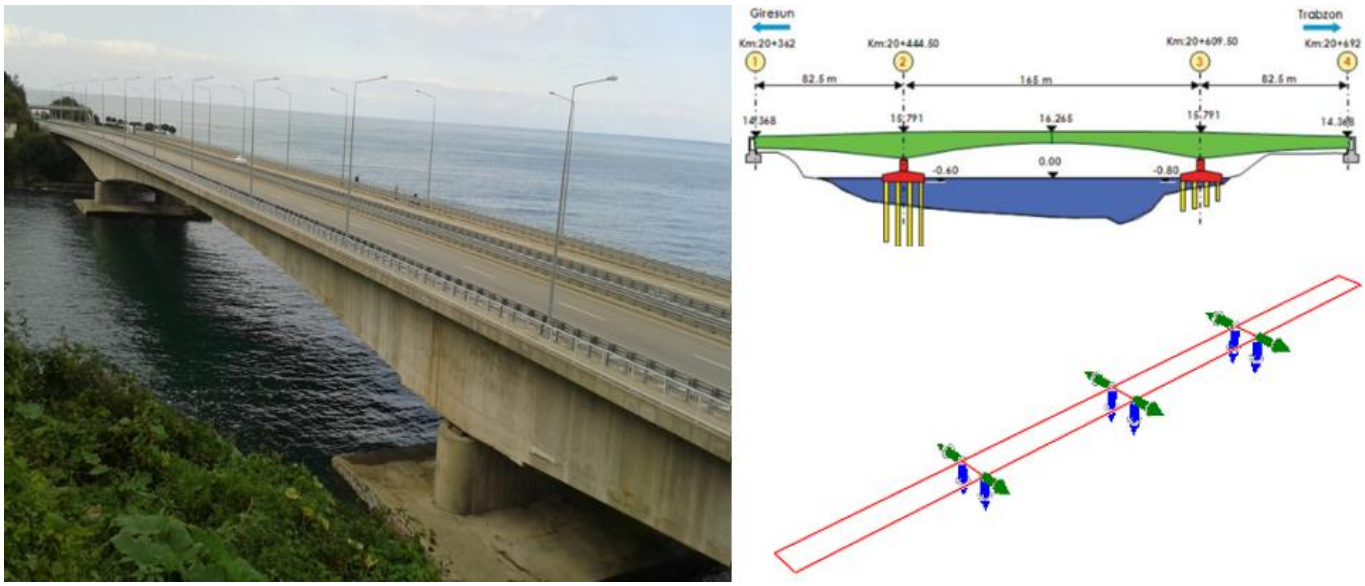

Figure 2. Gülburnu Highway Bridge.

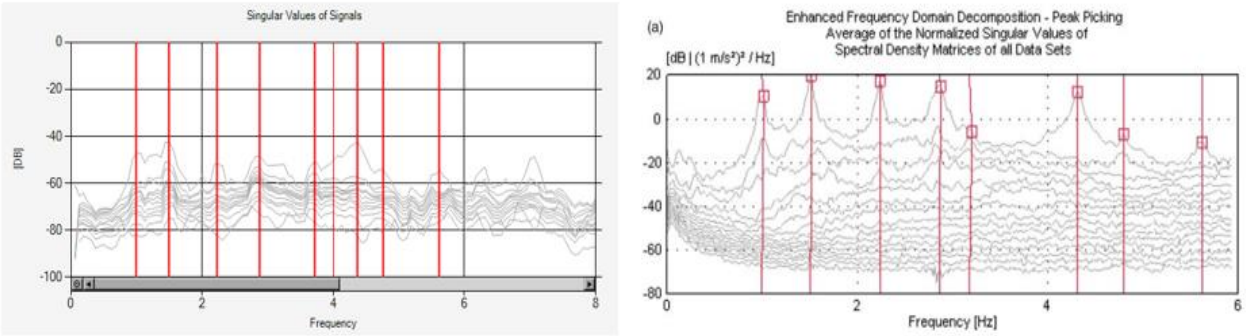

a) EFDD method

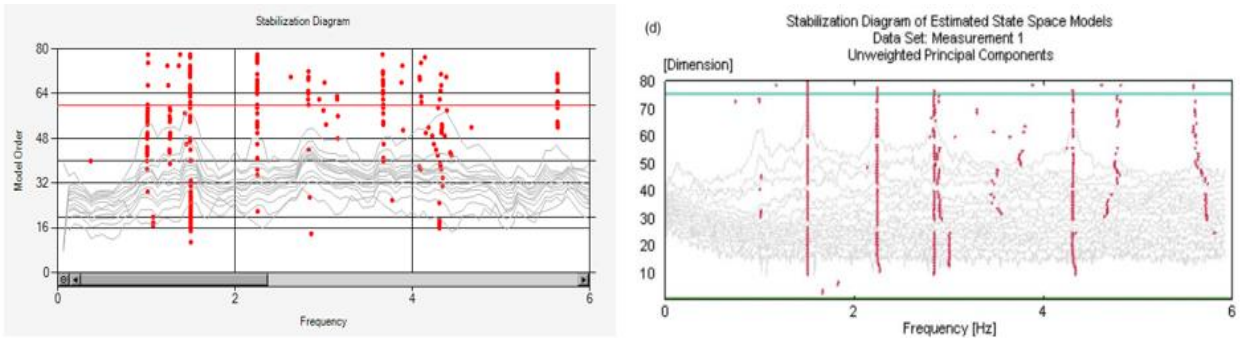

b) SSI method

Figure 3. Graphics obtained according to EFDD and SSI methods of Gülburnu Highway Bridge.

The frequency values obtained according to EFDD and SSI methods of Gülburnu Highway Bridge are given below. The results of the developed software are compared with the results of the Operational Modal Analysis [6] software. Table 1 shows the results and differences according to the EFDD and SSI method. The maximum differences obtained according to the EFDD and SSI method was 1.28%, 2.18%, respectively.

Table 1. Comparison of the results of Dynamic Modal and OMA software [6]

Mode No	EFDD			SSI		
	Dynamic Modal	OMA	Diff. (%)	Dynamic Modal	OMA	Diff. (%)
1	0,989	0,994	0,51	1,010	0,997	-1,28
2	1,489	1,508	1,28	1,492	1,505	0,87
3	2,223	2,238	0,68	2,248	2,238	-0,44
4	2,877	2,860	-0,59	2,790	2,850	2,15
5	3,174	3,175	0,03	3,12	3,188	2,18
6	4,362	4,314	-1,10	4,338	4,335	-0,07
7	4,754	4,793	0,82	----(*)	4,848	----
8	5,610	5,618	0,14	5,635	5,626	-0,16
(*) The frequency value of the related mode could not be obtained.						

3. DYNAMIC UPDATE

Comparison of experimental dynamic characteristics and finite element analysis results, ability to update finite element model under uncertain parameters, damage zone and damage level / severity can be evaluated by performing damage determination. In order to provide ease of operation, finite element model files (log file, s2k file etc.) created using different software can be easily transferred to the software. In this way, modal analysis results and dynamic characteristics can be obtained by extracting model coordinates and structural analysis parameters from the data file and using the created element matrices. By overlapping the results of the finite element model with the experimental results (especially the mode shapes), the differences between the dynamic characteristics can be calculated or the ratio of the fit can be calculated together with the MAC (Modal Assurance Criteria) and COMAC (Coordinate Modal Assurance Criteria). The improved finite element models obtained as a result of the sensitivity analysis can be transferred back to the desired finite element calculation programs. Figure 4 shows the login menu of the Dynamic Update software. The views of the modeling types made in the Dynamic Update software are given in Figure 5.

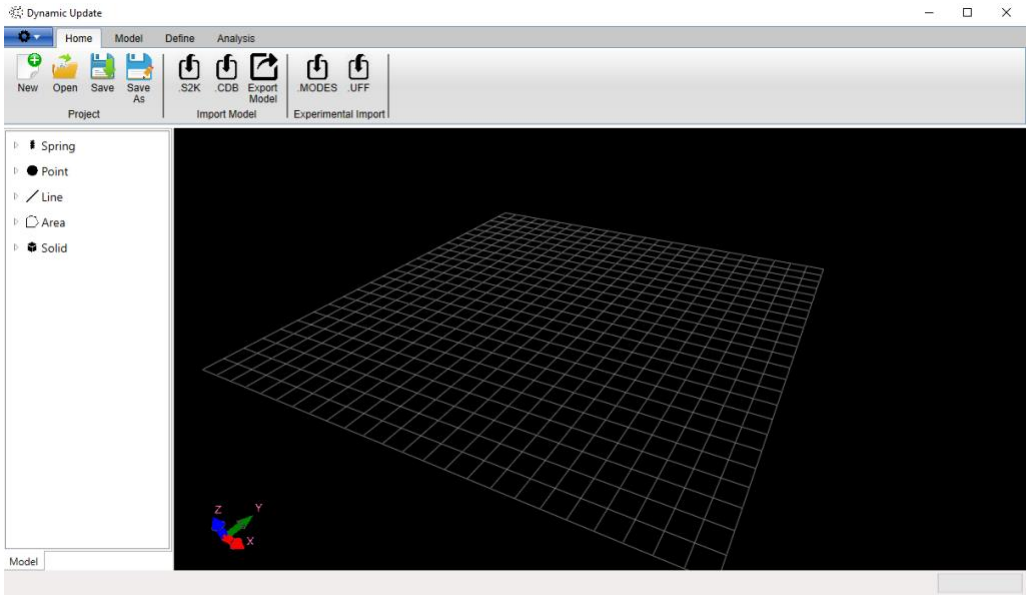

Figure 4. Login menu of Dynamic Update software.

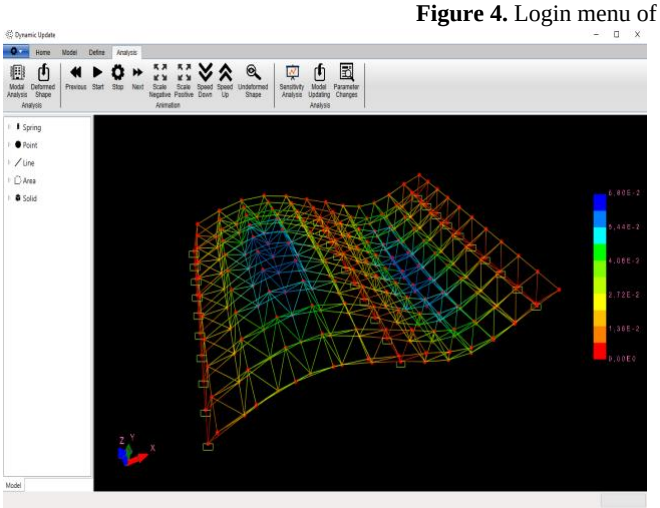

a) Frame elements

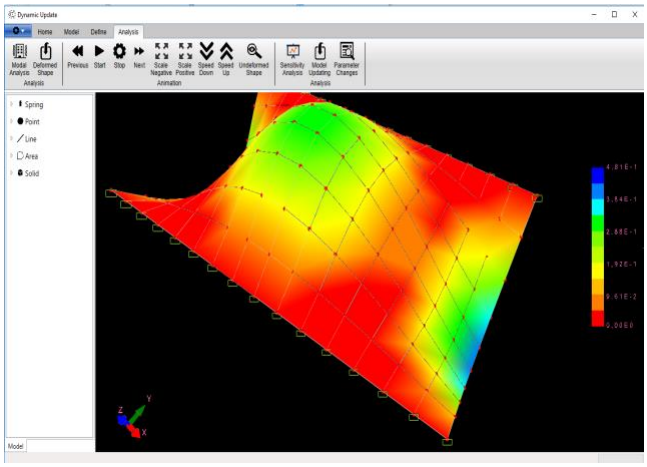

b) Area elements

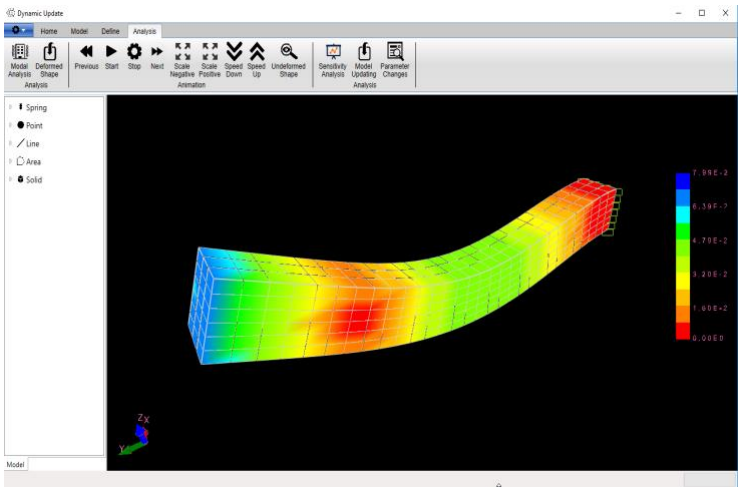

c) Solid elements

Figure 5. Some views to modeling types developed in the Dynamic Update software.

As a sample, damage assessment was made using the scaled Type-1 Arch Dam. The finite element model of the arch dam is given in Figure 6. The laboratory model, Type-1 Arch Dam, was damaged and experimental measurements of the damaged model were taken (Sevim, 2010) (Figure 7).

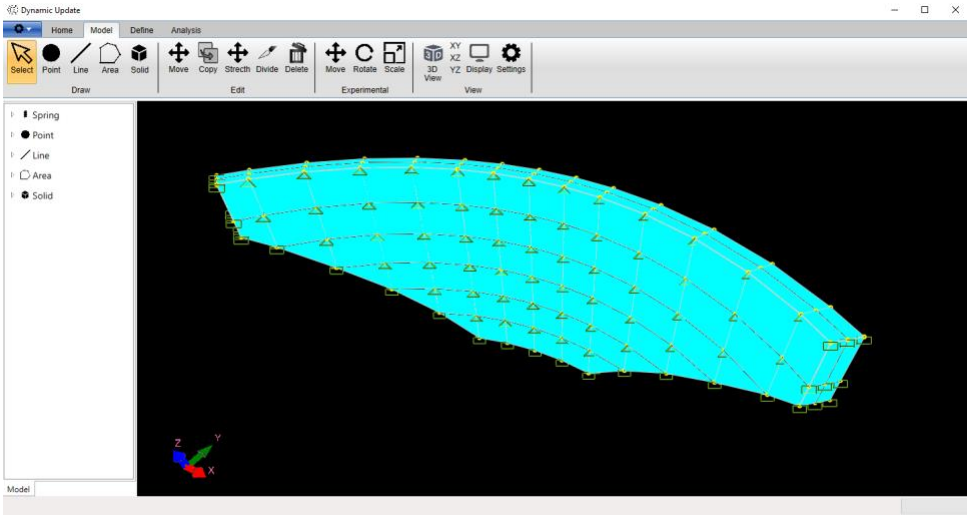

Figure 6. Finite element model of Tip-1 Arch Dam.

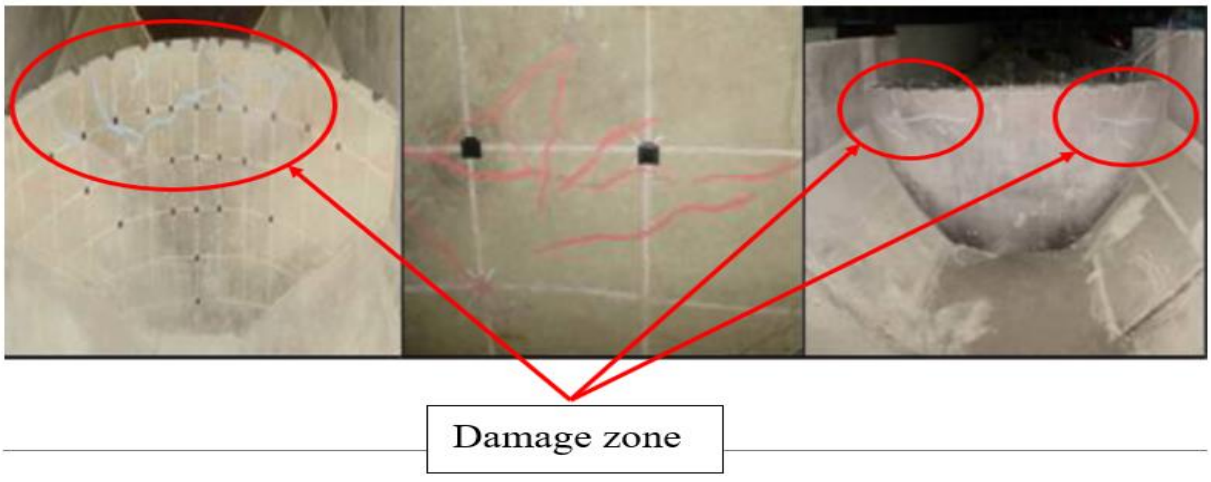

Figure 7. Experimental damage zones of Type-1 Arch Dam.

Elasticity Modulus changes of the elements that have been updated locally of scaled Type-1 Arch Dam by using Bayesian Parameter Estimation Method based on sensitivity are given in Figure 8. It was seen that the results obtained were compatible with the experimental ones.

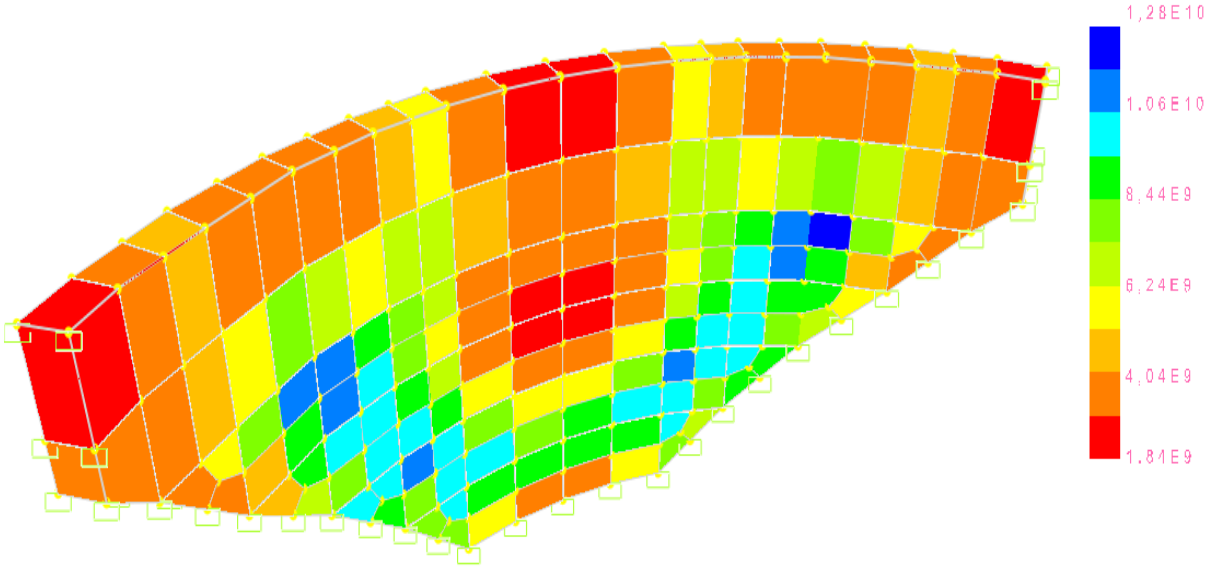

Figure 8. Numerical damage zones of Type-1 Arch Dam.

4. CONCLUSION

Foreign-sourced software requires high costs for important experimental work fields of civil engineering. With the help of domestic software, it is aimed that all academicians and researchers can reach the development of our country and these software with a lower budget. Dynamic Modal software for obtaining Experimental Modal Analysis results and Dynamic Update software for Model Update were developed. It was observed that the results obtained in the samples made within the scope of this study are compatible with the literature.

5. REFERENCES

1. Friswell, M. I., Mottershead, J. E. (1995). Finite element model updating in structural dynamics, solid mechanics and its applications, Kluwer Academic Publishers Group, 1-286, ISBN 978-0-7923-3431-6.

2. El-Borgi, S., Smaoui, H., Cherif, F., Bahlous, S., Ghrairi, A. (2004). Modal identification and finite element model updating of a reinforced concrete bridge, Emirates Journal for Engineering Research, 9(2), 29-34.

3. Modak, S. V., Kundra, T. K., Nakra, B. C. (2002). Comparative study of model updating methods using experimental data, Computers and Structures, 80(5-6), 437-447.

4. Jaishi, B., Ren, W. (2005). Structural finite element model updating using ambient vibration test results, Journal of Structure Engineering, ASCE, 131(4), 617-628.

5. Bayraktar, A., Altunışık, A.C., Sevim, B., Türker, T. (2007). Modal testing and finite element model calibration of an arch type steel footbridge, Steel and Composite Structures, 7(6), 487-502.

6. OMA. (2006). Release 4.0. Computer Software. Structural Vibration Solution, Aalborg, Denmark.

DOI: 10.38061/idunas.851853

IDUNAS	NATURAL & APPLIED SCIENCES JOURNAL	2021 Vol. 4 No. 1 (22-29)

Experimental Modal Analysis and Structural Health Monitoring of the Double Curvature Deriner Arch Dam

Research Article

Ahmet Can Altunışık[1*], Ebru Kalkan Okur[1*], Fatih Yesevi Okur[1*], Murat Günaydın[1*], Ali Fuat Genç[1*]

[1]Department of Civil Engineering, Karadeniz Technical University, Trabzon, Turkey.

Author E-mails
ahmetcan@ktu.edu.tr
ebrukalkan@ktu.edu.tr
yesevi@ktu.edu.tr
muratgunaydin@ktu.edu.tr
af.genc@ktu.edu.tr

*Correspondance to: Ahmet Can Altunışık, Department of Civil Engineering, Karadeniz Technical University, Trabzon, Turkey.
DOI: 10.38061/idunas.851853

Received: 01.01.2021; Accepted: 06.03.2021

Abstract

Arch dams have delicate sections thanks to their curvature. The fact that these dams are large, costly and construction takes many years increases the importance of the structure. Mistakes and / or accidents that may occur during the construction of such structures may occur major loss of life and property. Considering the volumes, masses and slenderness of arch dams, they can be significantly affected by dynamic forces such as changing water pressure, temperature, wind and earthquakes. The level of these effects and to what extent they affect the dam can be determined by the analysis to be made to finite element model created by computer. Since Finite Element Analysis is based on certain assumptions, the results obtained should be compared and / or verified with the results obtained by experimental methods. One of the most suitable methods preferred in many engineering structures is the experimental modal analysis method. Within the scope of the study, experimental vibration tests were carried out in order to evaluate and determine the structural behavior of the double curvature Deriner Arch Dam, which has a body height of 249m and a crest length of 720m. Experimental measurements were carried out with accelerometers placed in appropriate places in order to obtain the mode shapes of the dam. The dynamic characteristics of the dam were determined using OMA software. The first seven natural frequencies of the Deriner arch dam were obtained in the range 1.60-4.10Hz. As a result of the negotiations with the DSI 26th Regional Directorate, the acceleration data obtained from the existing accelerometer system of the dam was instantly taken and a continuous monitoring process was initiated. This data was transferred to the web-based monitoring site and a structural condition monitoring platform was created.

Keywords: Deriner arch dam, Experimental modal analysis, Structural health monitoring.

1. INTRODUCTION

Historical buildings, bridges, high-rise buildings and dams are important engineering structures of strategic importance. These structures have different features with their usage areas, aesthetic appearance, their surroundings and their location, and there are many different examples in our country. Most of these structures, which have many variable parameters such as different material properties, construction techniques and ground properties from the first periods, have survived despite changing conditions and are still operating, and some of them are waiting to succumb to time and disappear.

Our country is home to many structures in terms of building diversity and has various dam structures built in order to process many rivers and streams it has without harming the nature and to meet the energy needs of humanity. For the dam planned to be built, it is necessary to determine the most suitable dam type (weight, earth fill, rock fill, clay core, arch braces, concrete front face, roller compacted and arch dams etc.) by considering regional characteristics, purpose of use and economic situation.

Considering the volumes, heavy masses and slenderness of arch dams, they can be significantly affected by dynamic forces such as changing water pressure, temperature, wind and earthquakes. The behavior of the structure under these dynamic effects is determined depending on the dynamic characteristics defined as natural frequency, mode shape and damping ratio. Today, dynamic characteristics are determined analytically as a result of modal (free vibration) analysis of finite element models created according to element sizes, material properties and boundary conditions determined by considering the project data of linear structures. However, the parameters taken into account during the analysis may have changed due to reasons such as the loss of strength of the structure material over time, construction errors during the construction of the building, cracks, fatigue and support collapses caused by the different loads to which the building is exposed, and the dynamic characteristics of the building may have moved away from the project values over time. Therefore, it is thought that incorrect analysis results can be obtained by using analytically determined dynamic characteristics in determining the behavior of structures under earthquake and continuous dynamic loads. This idea has been emphasized in studies by many researchers [1-8]. Therefore, the dynamic characteristics of the structure should be determined by experimental methods as well as analytical methods. Since the Experimental Modal Analysis method is applied directly to the structure, the dynamic characteristics obtained reflect the current state of the structure.

Engineering structures continue to be used despite aging and deterioration far beyond their design life. Conventional control and monitoring techniques performed on these structures may produce inconsistent results. Besides, traditional inspection methods are very labor and time consuming. Therefore, new structural health monitoring systems should be developed that are automatic, highly sensitive, sensitive to minimal changes and cost effective [9]. Structural health monitoring is a continuous system description of a physical or parametric model of the building using time-dependent data [10]. Improvements in sensor placement and computational modeling allow important steps to be taken in the field of Structural Health Monitoring in the near future. A commonly used Structural Health Monitoring strategy is to perform a vibration analysis in which an intact (initial) model of the structure is compared with vibration response data collected from the physical structure. Differences between model estimates and monitoring data can be interpreted as structural damage [11]. In recent years, the management and security control of dams are based on automatic monitoring by used advanced technology. This situation allows the evaluation of the structural condition that changes over time and intervention in the structure in case of emergency in engineering structures of great importance [12-16].

In this study, it was aimed to develop a Web-based Structural Health Monitoring Portal to evaluate the structural condition of Deriner Arch Dam and to monitor its current status. Experimental modal analysis

test of Deriner Arch Dam, which is Turkey's highest dam is made. In addition, data from the existing accelerometer system in Deriner Dam has been transferred to the online Structural Health Monitoring platform. Thus, instant monitoring and storage of data is provided.

2. EXPERIMANTAL MODAL ANALYSIS OF DERINER ARCH DAM

Deriner Dam is a double curvature concrete arch dam and was built on the Coruh River. The body height from the foundation is 249.00m and the crest length is 720m. The dam construction, which started in 1998, was completed and in 2012 the water started to be kept. Experimental vibration tests have begun to be carried out in order to evaluate and determine the structural behavior of Deriner Arch Dam, which continues to produce electricity at full capacity, over the years and the structural behaviors it will show in the future. In the tests, cable accelerometers with single axis type B&K 8340 and a sensitivity of 10 V / g were used. The signals from the accelerometers were collected in a B&K 3560 type 17-channel data acquisition unit and transferred to PULSE [17] software. Dynamic characteristics were determined using OMA [18] software.

Ambient vibration tests were carried out under the effect of wind and water pressure in Deriner Arch Dam. The first measurement on Deriner Dam was carried out on 12 June 2019 with accelerometers placed at the crest level. Photographs of the experimental measurements made in the Deriner Arch Dam are given in Figure 1.

Figure 1. Some photos of the experimental measurements carried out in Deriner Arch Dam.

During the test, accelerometers were placed upstream-downstream of the dam crest. Because of the limited number of accelerometers and cable lengths, experimental measurements were taken by creating three different setup (Figure 2). Each setup was carried out by taking measurements with reference within itself (Figure 3). The distance between the accelerometers was determined as 45m and 9 accelerometers were used in setup 1 and 2, and 7 accelerometers were used in setup 3. At each measurement, measurements were taken for 30 minutes and signals were collected.

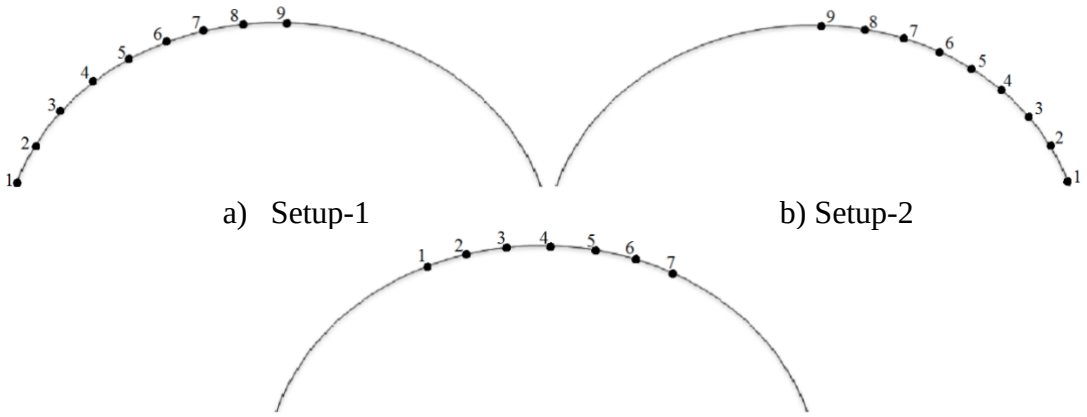

Figure 2. Schematic representation of the measurements made in the Deriner Arch Dam.

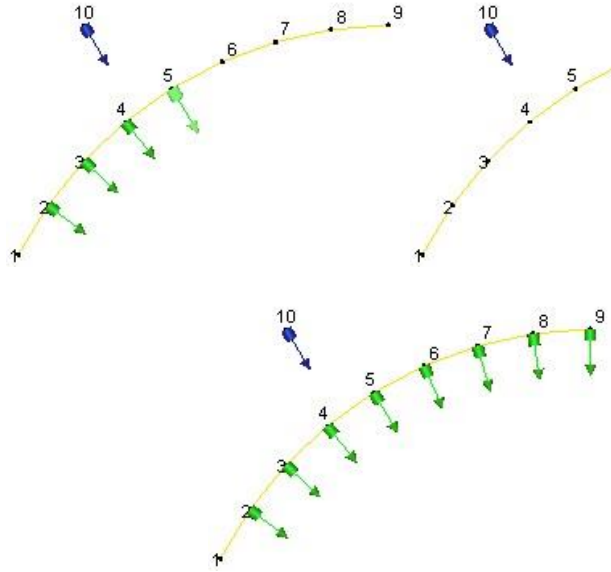

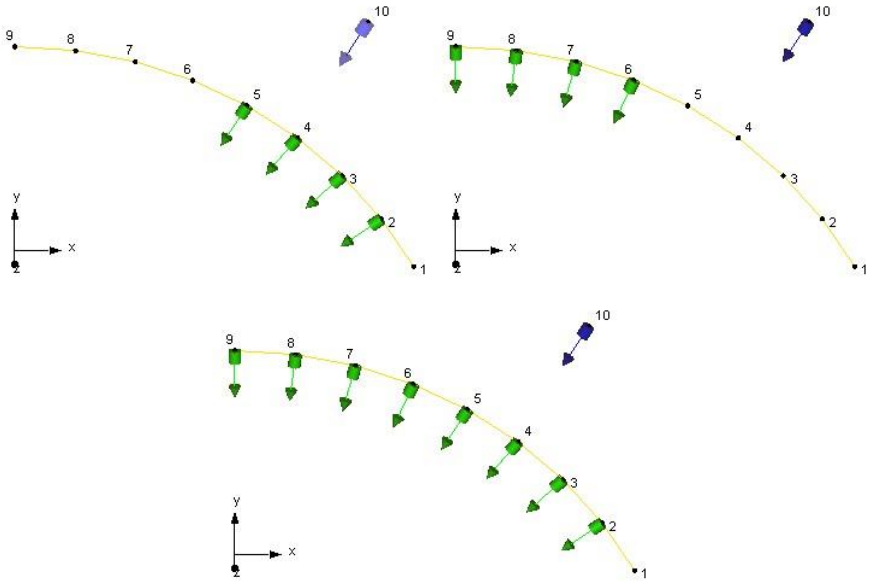

b) Setup-2

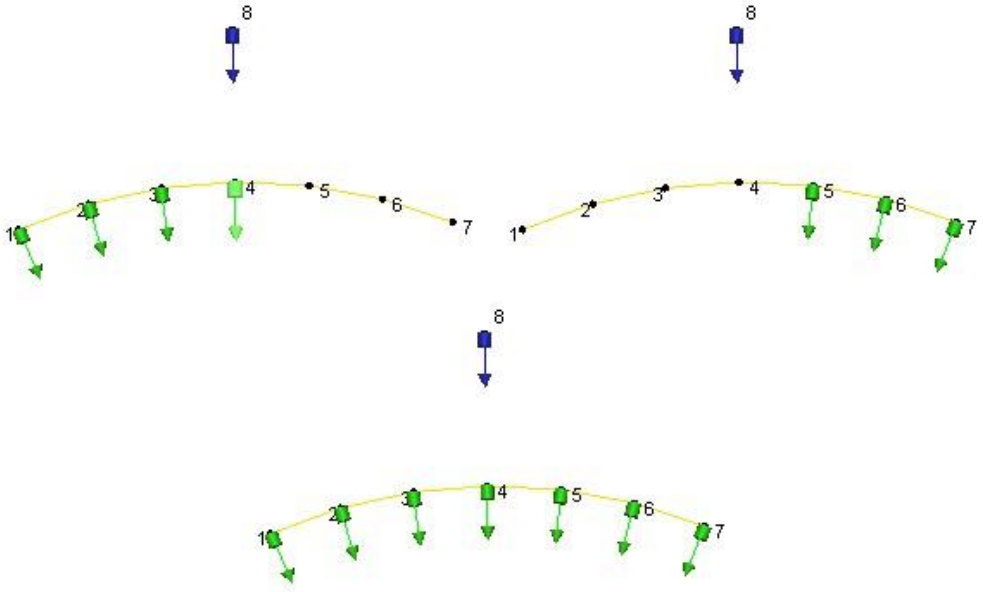

c) Setup-3

Figure 3. Accelerometer locations for each ambient vibration test.

Figure 4 shows the diagram obtained in the frequency domain according to the Enhanced Frequency Domain Decomposition (EFDD) methods from the ambient vibration tests of the Deriner dam. Table 1 shows the frequency values obtained from setup-1 and setup-3 of the Deriner Arch Dam's measurement dated 12/06/2019.

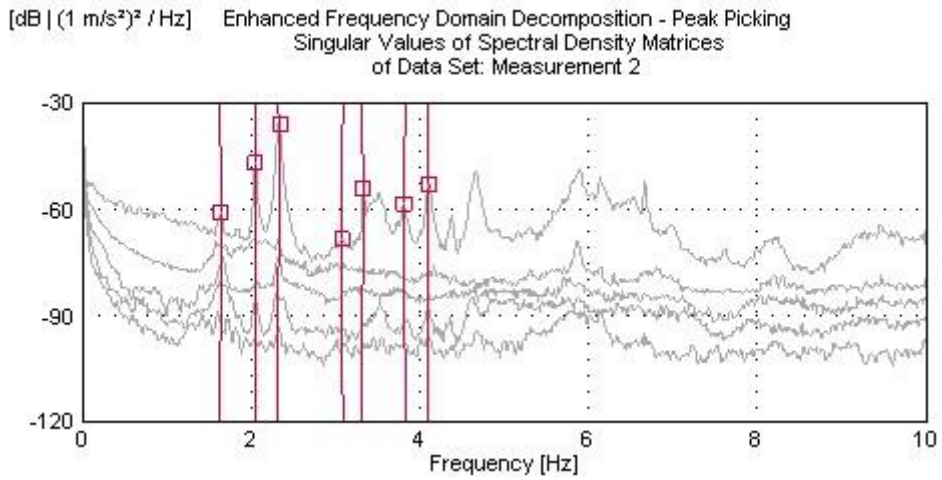

Figure 4. Singular value of spectral density matrices of Deriner Arch Dam.

Table 1. Frequency values obtained from setup-1 and setup-3 of Deriner Arch Dam's measurements dated 12/06/2019.

Mode No	Frequency Values (Hz)	
	Setup-1	Setup-3
1	1.638	1.638
2	2.052	2.158
3	2.310	2.286
4	3.090	3.057
5	3.322	3.498
6	3.831	3.950
7	4.105	4.098

3. STRUCTURAL HEALTH MONITORING OF DERINER ARCH DAM

Deriner Arch Dam currently has systems for monitoring structural health. However, existing measuring instruments allow only certain and insufficient data to be received. 5 accelerometers in Deriner Arch Dam record only 4sec data between 00:00:00 and 00:00:00 every night. Short-term measurement records are not sufficient for processing data and obtaining frequency values. For this reason, it was ensured that data from the current accelerometer system was continuously received and recorded 24/7 and transferred to the Structural Health Monitoring Portal prepared on a web-based. Figure 5 shows the interface of the website prepared.

Figure 5. Structural Health Monitoring website.

With this portal, it was ensured that the signal data received from the accelerometer can be monitored online and accessed on the desired date. Figure 6 shows the page where instantaneous acceleration data of Deriner arch Dam are obtained.

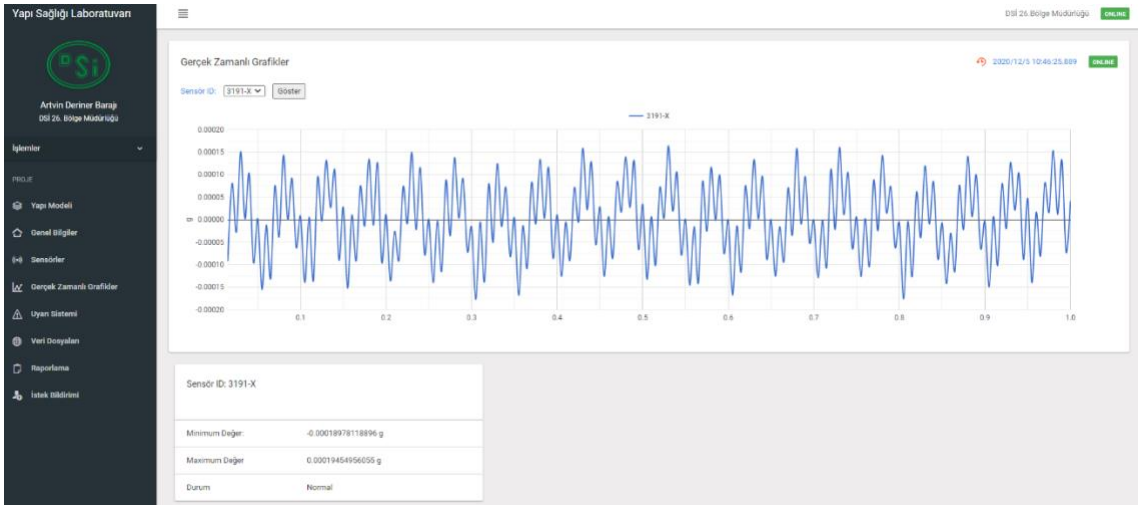

Figure 6. Instant acceleration data of Deriner Arch Dam.

4. CONCLUSION

In this article, studies carried out to evaluate the structural condition of Deriner Arch Dam and to continuously monitor its current situation are included. Experimental modal analysis tests of the double curvature Deriner Arch Dam built on the Coruh River were conducted. As a result of the experimental measurements, the frequency values of the first seven modes expressing the current state of the dam were obtained between 1.6Hz and 4.1Hz. Due to insufficient data collection in the existing structural health monitoring system in the dam, the acceleration data of the dam can be instantly transferred to the Web-based Structural Health Monitoring Portal prepared by improving the existing system. Acceleration data of the dam can be monitored and stored instantly with this web-based portal.

5. ACKNOWLEDGMENTS

We would like to thank the General Directorate of State Hydraulic Works (DSI in Turkish acronym) and the 26th Regional Directorate for granting the necessary permits for the experimental studies carried out at Artvin Deriner Dam.

6. REFERENCES

1. Chuntavan, C. (1993). Structural identification of steel stringer bridges for condition assessment, Doctoral Thesis, University of Cincinnati, Cincinnati, USA.

2. Womack, K. C., Halling, M. W. (1999). Forced vibration testing of the I-15 south temple bridge, Project Final Report, Report No: UT-99.15, Department of Civil and Environmental Engineering, Utah State University, Logan, Utah, USA.

3. Achter, J. L. (2000). Full-scale bridge bent condition assessment using forced-vibration testing, Master Thesis, Utah State University, Logan, Utah.

4. Inaudi, D., Casanova, N., Vurpillot, S., Glisic, B., Kronenberg, P., Lloret, S. (2000). Bridge deformation monitoring during enlargement and refurbishment works under traffic conditions, International Association for Bridge and Structural Engineering, IABSE, 16th Congress, Luzern, Switzerland.

5. Halling, M. W., Muhammad, I., Womack, K. C. (2001) Dynamic field testing for condition assessment bridge bents, Journal of Structural Engineering, ASCE, 127(2), 161-167.

6. Zhao, J., DeWolf, J. T. (2002) Dynamic monitoring of steel girder highway bridge, Journal of Bridge Engineering, ASCE, 7(6), 350-356.

7. Brownjohn, J. M. W., Moyo, P., Omenzetter, P., Lu, Y. (2003). Assessment of highway bridge upgrading by dynamic testing and finite-element model updating, Journal of Bridge Engineering, ASCE, 8(3), 162-172.

8. Kim, J. T., Stubbs, N. (2003). Nondestructive crack detection algorithm for full-scale bridges, Journal of Structural Engineering, ASCE, 129(10), 1358-1366.

9. Reagen, D., Sabato, A., Christopher N. (2017). Unmanned aerial vehicle acquisition of three-dimensional digital image correlation measurements for structural health monitoring of bridges, Nondestructive Characterization and Monitoring of Advanced Materials, Aerospace and Civil Infrastructure, 10.1117/12.2259985.

10. Brownjohn, J. M. W. (2009) Structural healt monitoring of civil infrastructure, Mathematical, Physicaland Engineering Sciences, 365, 589-622.

11. Buren, K. V., Reilly J., Neal K., Edwards H., Hemez F. (2017). Guaranteeing robustness of structural condition monitoring to environmental variability, Journal of Sound and Vibration, 386, 134-148.

12. Pereira, S., Magalhaes, F., Cunha, A., Gomes, J., Lemos, J. V. (2019). Installation and results from the first 18 months of operation of the dynamic monitoring system of Baixo Sabor Arch Dam, 6th International Symposium on Life-Cycle Civil Engineering (IALCCE), 1167-1173, Ghent, Belgium.

13. Oliveira, S., Alegre, A. (2019). Seismic and structural health monitoring of dams in Portugal, Seismic Structural Health Monitoring: From Theory to Successful Applications, Springer International Publishing AG, 87-113.

14. Oliveira, S., Alegre, A. (2020). Seismic and structural health monitoring of Cabril Dam. Software development for informed management, Journal of Civil Structural Health Monitoring, 10(5), 913-925.

15. Liseikin, A. V., Seleznev, V. S., Adilov, Z. A. (2020). Monitoring of the natural frequencies of Chirkey Arch Dam, Magazine of Civil Engineering, 96(4), 15-26.

16. Hsu, T. Y., Valentino, A., Liseikin, A., Krechetov, D., Chen, C. C., Lin, T. K., Wang, R. Z., Chang, K. C., Seleznev, V. (2020). Continuous structural health monitoring of the Sayano-Shushenskaya Dam using off-site seismic station data accounting for environmental effects, Measurement Science and Technology, 31(1), 015801.

17. PULSE, (2006). Analyzers and Solutions, Release 11.2. Bruel and Kjaer, Sound and Vibration Measurement A/S, Denmark.

18. OMA, (2006). Release 4.0, Computer Software. Structural Vibration Solution, Aalborg, Denmark.

DOI: 10.38061/idunas.853356

IDUNAS	NATURAL & APPLIED SCIENCES JOURNAL	2021 Vol. 4 No. 1 (30-37)

An Image Segmentation Method for Wound Healing Assay Images

Research Article

Yusuf Sait Erdem[1*], Özden Yalçın Özuysal[2*], Devrim Pesen Okvur[2*], Behçet Uğur Töreyin[3*], Devrim Ünay[1*]

[1]Department of Electrical and Electronics Engineering, İzmir Demokrasi University, Karabağlar, İzmir, Turkey.

[2]Department of Molecular Biology and Genetics, İzmir Institute of Technology, Urla, İzmir, Turkey.

[3]Istanbul Technical University Informatics Institute, İTÜ Ayazağa Kampüsü, Sarıyer, İstanbul, Turkey.

Author E-mails:
yusufsaiterdem@gmail.com
ozdenyalcin@iyte.edu.tr
devrimpesen@iyte.edu.tr
toreyin@itu.edu.tr
devrim.unay@uzem.idu.edu.tr

*Correspondance to: Yusuf Sait Erdem, Department of Electrical and Electronics Engineering, İzmir Demokrasi University, Karabağlar, İzmir, Turkey.
DOI: 10.38061/idunas.853356

Received: 04.01.2021; Accepted: 05.04.2021

Abstract

Wound healing assays are important for molecular biologists to understand the mechanisms of cell migration. For the analysis of wound healing assays, accurate segmentation of the wound front is a necessity. Manual annotation of the wound front is inconvenient since it is time-consuming and annotator-dependent. Thus automated, fast, and robust solutions are required. There are several image processing techniques proposed to fulfill this need. However, requirement for specification of optimal parameters, the need for human intervention, and the lack of high accuracy emerge as the downfalls for most of them. In this study we have proposed a novel method to overcome these difficulties.
Keywords: Image segmentation, quantification, wound healing assay, collective cell migration, phase-contrast microscopy.

1. INTRODUCTION

Wound healing assay in vitro became a widespread technique to analyze many complicated biological processes such as immune system activation, spread of tumor, and metastasis as well as embodiment of tissues. Advances in the automation of microscopic imaging has boosted extraction of more data from wound healing assays [4, 6-7]. Segmentation of such excessive amount of data by hand is tedious, time consuming, and subjective. Therefore, many automated methods for the segmentation of wound healing assay images are proposed in the literature. However, the need for more accurate, robust, and practical methods still resides.

There are several widely used tools available for the segmentation of wound healing assays such as MRI Wound Healing Tool macro developed for ImageJ [10] and Cell 1 Image Velocimetry (CIV) [9]. In the MRI Wound Healing Tool plugin, users should tune the parameters such as the preferred method, radius of structuring element used in morphological opening, and minimum wound size. In the segmentation method of CIV, parameters such as scaling factor, radius of local contrast normalization, thresholds for local and global filtering, and kernel size should be set by the user to obtain an adequate segmentation result.

Deep learning methods are also utilized for wound healing assay image segmentation [11]. While these methods may maintain high accuracy, they need a training process with a decent amount of annotated data.

Matsubayashi et al. introduced 'White wave' tool which suggests a novel measure to take account instead of direct frontier distances for wound closing analysis [1]. The tool first takes difference image of consecutive frames of wound closing footage. The difference image is computed by taking absolute value of difference of each corresponding pixel. Then calculates a histogram of resulting difference image's vertical average intensities corresponding to x-axis. 'x' coordinates of two peaked average intensity values of histogram are taken as positions of wound edges assuming that the wound closing image has two vertical sides of wounds. Matsubayashi et al. proposes that average value is more robust and contains more information than direct frontier distances. That average value represents the x location of wound edge, shows movement of wound sides even after complete closure of the wound which is claimed that is more consistent to the domain knowledge [1]. Even though this method unveils movement information, it does not produce data to calculate an actual wound closure speed metric nor a wound area metric.

The TScratch wound analysis tool published by Gebäck - Tobias et al. uses discrete curvelet transformation together with morphological operations to segment wound surfaces [2]. Curvelet transformation is used for detection of edges and elimination of noises in a wound closing assay image. At first, curvelet magnitude image is generated by using 2 scale levels where wound surface edges are visible. Then morphological opening is applied. Two peak areas on curvelet histogram are taken as true edges and the rest is assumed as noise edges. Small areas are considered as noise and removed on curvelet transformed image after a morphological opening operation. Finally, an erosion operation is applied to resulting image [2]. TScratch method finds scale-level parameter automatically but that critical parameter is needed to be empirically adjusted by user on same cases for good segmentation result.

Suarez-Arnedo et al. developed a wound healing assay analysis tool by using contrast enhancement and variance filtering [3]. The tool takes radius of variance filter, binarization intensity threshold and saturation percentage as user inputs for each frame in video input. The tool first enhances contrast using saturation percentage parameter than applies variance filter. Thresholds image for binarization. Then applies erosion to remove small, independent particles and hole filling operation. Resulting, largest component is taken as the empty wound area. Width deviation of the wound is calculated by taking horizontal distances across the detected wound edges. The tool also calculates the wound area in pixels as well as the empty wound area to cell edge area ratio [3].

A high throughput wound healing assay method for quantitative output is suggested by Zordan et al. where an instrument for reproducible wounding and entropy filtering for segmentation is used. The bright field image collected from the assay is cropped using a user defined input to omit some unnecessary regions. An 11x11 pixel sized entropy filter is applied and thresholded with an input value of between 0.5 and 0.85, generally. 2 The resulting binary image is inverted, and a morphological opening operation is applied to remove small wound regions. Dilation is applied after for smooth surfaces. To generate a connected wound area, a morphological closing applied with a 5x5 pixel sized oval kernel and a morphological fill is applied.

Detected cell regions those are touching to single border of the image are discarded. Area of the empty wound region on entropy filtered image is used to calculate wound closing percentage during the assay [4].

Topman et al. calculated wound area by segmenting wound assay images using two separate standard deviation windows [5]. One of these windows has "big" size for detecting large shapes and the other one has small size for keeping small details on the edges of cell regions. After standard deviation is applied with "big" windows, a peak point in histogram of intensities is detected. Half of this intensity value is used as threshold value for the resulting image. After obtaining the binary image, dilation is applied by a rectangular kernel whose size is half of the big window size. Same procedure is applied with the "small" windows size except dilation and the resulting images are combined. Morphological closing and opening operations applied to combined image using kernel with size of the small window. Since the sizes of small and big windows are determined as constant values in real metrics, real scale of the assay images should be known in this method. Garcia et al. introduced a similar method, but they have used a single window for standard deviation and morphological filling operation additionally [8].

These methods work successfully under certain conditions but, they depend on many critical parameters such as kernel size [3, 5, 8], saturation rate [3-4], and scale-level [2]. To achieve high and consistent accuracy on various conditions, they require human intervention for the determination of optimal parameter set, which makes them difficult to use. Our method, on the other hand, depends on a single parameter and thus emerges as a more robust solution. Even if this single parameter of ours needs to be reset to obtain premium accuracy on a limited number of cases, it can be approximately determined by analyzing the width of cell pixels present in the assay.

2. METHODOLOGY

Experimentation and Data

The experiments and the image acquisition of the in-vitro wound healing assays employed in this study are realized at the Molecular Biology and Genetics Department of İzmir Institute of Technology – Non-invasive breast cancer cell line MCF7 cells in epithelial morphology are planted in 6-well petri dishes and allowed to attach for 24 hours. The wound was artificially created prior to imaging by scraping the surface in a line with the tip of a yellow pipette. For the imaging petri dishes are placed in the incubation room of the Leica SP8 microscopy system providing constant temperature of 37°C and 5% CO2. Phase-contrast image acquisition is performed using a Leica SP8 microscopy system with 10x objective at every 60 minutes throughout a 48-hour duration. The images acquired have 1920x1440 pixels resolution.

Manual Segmentation

Wound healing assay data is annotated manually for the evaluation of the methods. Contour of each empty wound region is annotated as polygons using the online image annotation tool Supervisely [12]. Annotations are realized by a single annotator under 3 the supervision of molecular biologists. For this study, four wound healing assay videos are annotated, corresponding to a total of 65 frames in 1920x1440 pixel resolution. Number of annotated frames per assay varies depending on the wound closure speed.

Automated Segmentation of Wound Healing Assays

Our method at first takes spatial derivative of the 2D input image. Then it applies smoothing by convolving the difference image with Gaussian kernel and binarizes the result by nonzero pixels. Width of the Gaussian kernel is a constant parameter which is loosely equal to the width of the smallest cell in input

images. For our experiments, 25 pixels is taken as smallest cell width in pixels. Small blobs are removed after dilating the resulting image, and erosion is applied on the outcome. Isolated cell areas touching a single border of the image are eliminated, as in Zordan et al.'s method [4], since they do not belong to any side of the wound. The biggest detected empty area assumed to be the open wound area. Following the segmentation of the first frame, consecutive frames are analyzed in a similar manner except, not only the biggest detected empty area is returned but other empty regions are taken in account too. Remaining empty regions are sorted according to their areas. To determine these regions as empty region, shrinkage rate of the biggest region is calculated by dividing current biggest empty area with the previous one. This shrinkage rate is multiplied by current biggest empty area. Regions having larger size than the calculated area are assigned as the wound region if the total area is less than the one before as shown in Figure 1.

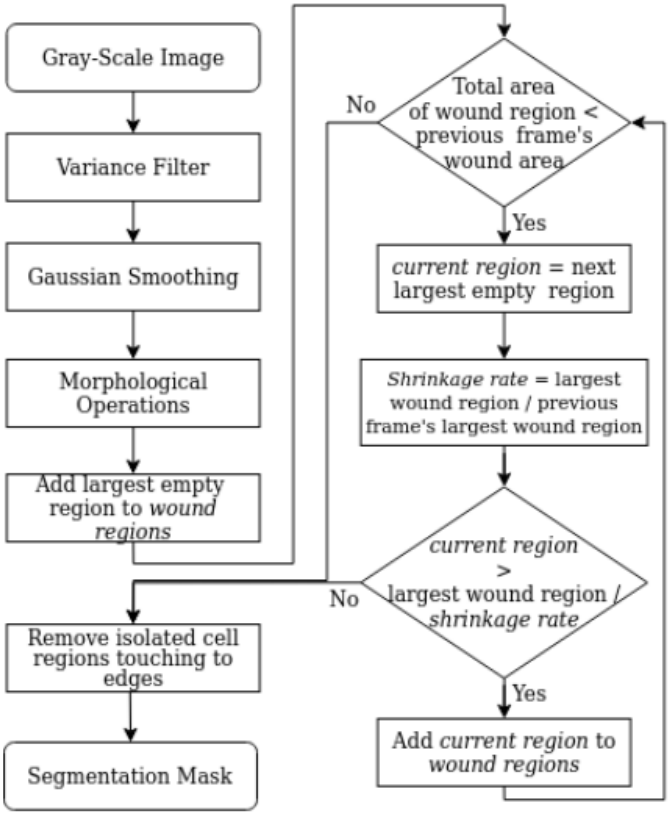

Figure 1. Flowchart of our image segmentation method for wound healing assay images.

Once the wound image is segmented, the two opposite borders (wound fronts) of the wound opening are extracted. For that purpose, a bounding box is fitted to the segmented wound opening and split into two vertical halves using a midline extraction approach as shown in Figure 2.

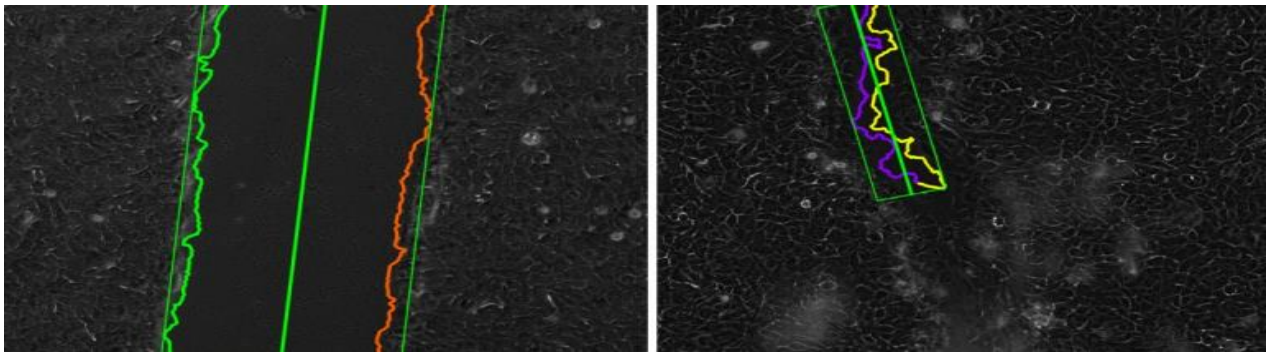

Figure 2. Identification of the wound fronts or borders.

Metrics Used for Quantification

For the evaluation of the segmentation accuracy obtained by the methods experimented, Dice coefficient score is employed as:

$$DiceScore(R_g, R_p) = \frac{2 * |R_g \cap R_p|}{|R_g| + |R_p|} \quad (1)$$

where Rg and Rp correspond to the ground truth and predicted regions, respectively. To quantify wound closure from the assay data, the Mean Surface Distance is calculated on the detected wound surfaces at each frame as well as the rate of the area occupied by the open wound region. Mean Surface Distance measures the distance between two surfaces by averaging the minimum distances across surfaces based on the following formula:

$$MSD(S1, S2) = \frac{1}{N_{S1} + N_{S2}} \left(\sum_{i=1}^{N_{S1}} \left| d_i^{S1 \to S2} \right| + \sum_{i=1}^{N_{S2}} \left| d_i^{S2 \to S1} \right| \right) \quad (2)$$

where S1 and S2 are the frontiers of wound regions, NS1 and NS2 are the point counts of the surfaces, and d is the 2D Euclidean distances.

3. EXPERIMENTAL RESULTS AND DISCUSSION

We have compared the performance and robustness of our method with other automated solutions present in the literature using four annotated wound healing assay data. Figure 3 demonstrates exemplary frames from one of the assays together with the corresponding ground truths and the related Dice scores of the methods per frame. As observed in the graphical result (Figure 3, top), all methods show high accuracy in the beginning of the experiment (i.e. at the initial frames) while as the wound healing occurs (i.e. towards later frames) accuracies of the methods decline. We see that TScratch is the worst performer overall, whereas our method achieves similar performance overall with PyScratch. Figure 4 graphically presents the average Dice scores of each method, with the corresponding standard deviations, over all four annotated essays. As seen, our method outperforms its rivals in average Dice score. We observe that all methods depict large standard deviations, which can be attributed to the performance variations due to the increased difficulty in wound segmentation as the healing progresses. Only Topman et al.'s method has a slightly lower standard deviation than our's, but that method has the lowest average dice score.

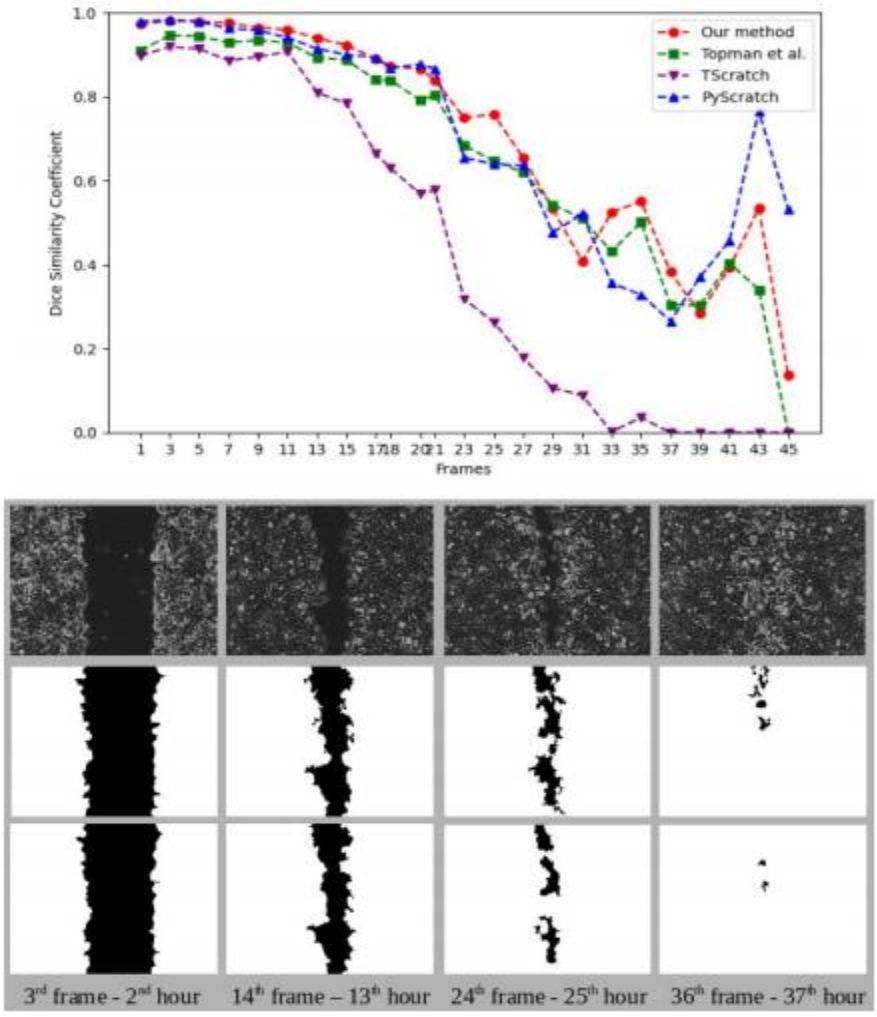

Figure 3. Top: Performance comparison of the methods based on their Dice similarity coefficients per frame. Second row: Exemplary frames from a wound healing assay data. Third row: Corresponding ground truth segmentations. Fourth row: Corresponding segmentation results of our proposed method.

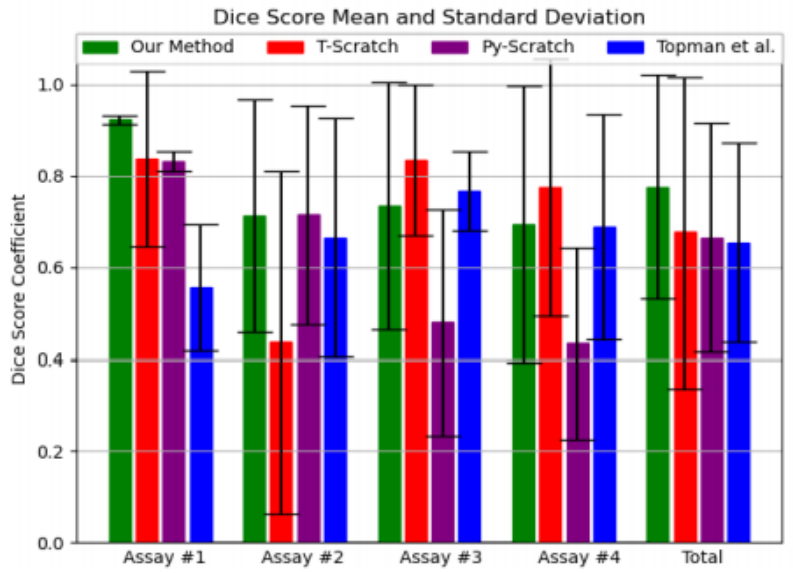

Figure 4. Performance comparison of the methods based on their average Dice similarity coefficients and standard deviations per assay as well as overall (i.e. Total).

The wound surface distance together with the area of the open wound region is computed and displayed for each frame to allow for better representation of the wound healing. Figure 5 shows a visual example of the distances computed from the opposite wound fronts (left) and the temporal change in the mean surface distance (right). We see 6 gradual decline in the mean surface distances of the wound opening, which can be attributed to wound repair.

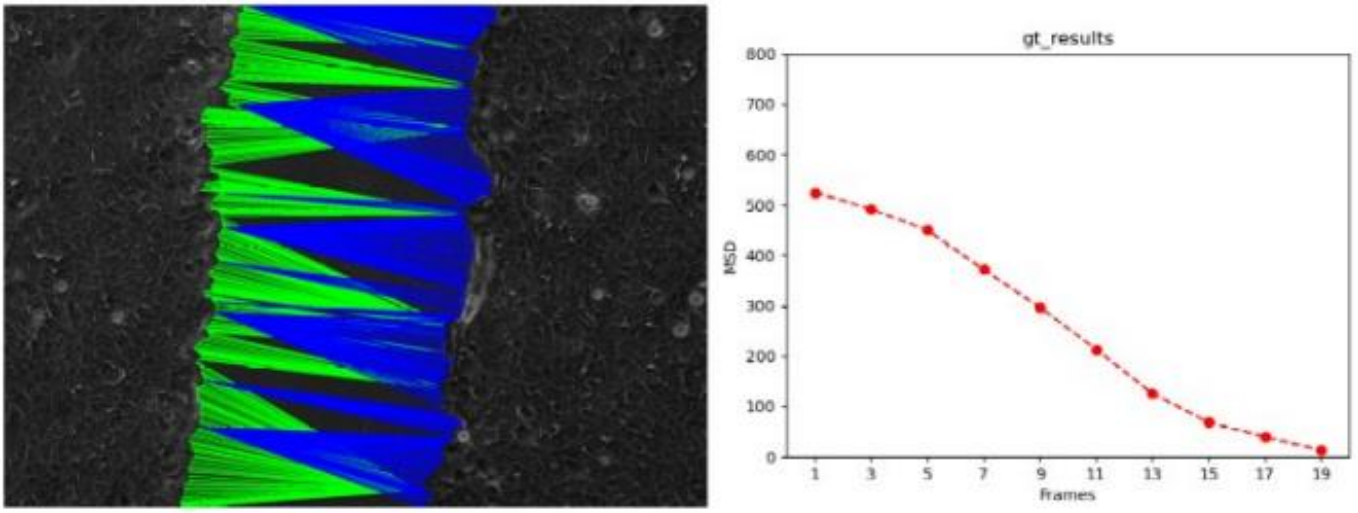

Figure 5. Left: Visualization of closest surface distances. Right: Mean surface distance graph of a wound healing assay.

4. CONCLUSION

Wound healing assays are frequently employed by molecular biologists to study collective cell migration and cell-cell interaction. Routinely, these assays are continuously monitored by optical microscopy and image series are generated for their further analyses. Segmentation of the wound area from these image series is a critical step for the analysis and evaluation of the assay results. As manual segmentation is tedious, time consuming and subjective, automated solutions are needed. For this purpose, in this study we prosposed an automated, robust, and accurate solution for segmenting wound healing assay data. Comparison with the state-of-the-art methods, as quantified on several expert-annotated real wound healing assay data using Dice overlap and surface distance metrics, showed that our proposed solution achieves higher and consistent accuracies, and thus emerges as a suitable alternative for the quantitative analysis of in-vitro wound healing assays.

5. ACKNOWLEDGMENTS

This work is supported by the Scientific and Technological Research Council of Turkey (Tübitak) under grant no 119E578.

6. REFERENCES

1. Matsubayashi, Y., William R., Paul M. (2011)., White wave analysis of epithelial scratch wound healing reveals how cells mobilise back from the leading edge in a myosin-II-dependent fashion., Journal of cell science 124.7: 1017-1021.

2. Gebäck, T. (2009). et al., TScratch: a novel and simple software tool for automated analysis of monolayer wound healing assays: Short Technical Reports., Biotechniques 46.4: 265-274.

3. Suarez-Arnedo, A. (2020). et al., An image J plugin for the high throughput image analysis of in vitro scratch wound healing assays, bioRxiv.

4. Zordan, Michael D. (2011). et al., A high throughput, interactive imaging, bright-field wound healing assay., Cytometry Part A 79.3: 227-232.

5. Topman, G., Orna S., and Amit G. (2012). A standardized objective method for continuously measuring the kinematics of cultures covering a mechanically damaged site., Medical engineering & physics 34.2: 225-232.

6. Grada, A. (2017(et al., Research techniques made simple: analysis of collective cell migration using the wound healing assay., Journal of Investigative Dermatology 137.2: e11-e16.

7. Huang, K., and Robert F. M. (2004). From quantitative microscopy to automated image understanding., Journal of biomedical optics 9.5: 893-913.

8. Garcia, F., Vladimir Fernanda G., and B. de Jesus M. (2020). PyScratch: an ease of use tool for analysis of Scratch assays., Computer Methods and Programs in Biomedicine: 105476.

9. Milde, F. (2012). et al., Cell Image Velocimetry (CIV): boosting the automated quantification of cell migration in wound healing assays., Integrative Biology 4.11: 1437-1447.

10. Wound healing image segmentation tool: http://dev.mri.cnrs.fr/projects/imagejmacros/wiki/Wound_Healing_Tool

11. Mayalı, B. (2020). et al., Automated Analysis of Wound Healing Microscopy Image Series-A Preliminary Study., 2020 Medical Technologies Congress (TIPTEKNO). IEEE.

12. Online image annotation tool: https://supervise.ly

DOI: 10.38061/idunas.758764

IDUNAS	NATURAL & APPLIED SCIENCES JOURNAL	2021 Vol. 4 No. 1 (38-51)

Microbial Activities and Physicochemical Properties of Pesticide Treated Soils and Waters

Research Article

Sebiomo Adewole[1*], Banjo F. Mary[1*]

[1]Department of Biological Sciences, Tai Solarin University of Education Ijagun, Ijebu-Ode.

Author E-mails
rev20032002@yahoo.com
*Correspondance to: Sebiomo Adewole, Department of Biological Sciences, Tai Solarin University of Education Ijagun, Ijebu-Ode.
Tel: +234812263934
DOI: 10.38061/idunas.758764

Received: 26.06.2020; Accepted: 24.11.2020

Abstract

The aim of this study is to determine microbial activities and physicochemical properties of pesticide treated soils and waters . Nutrient agar (NA)and Potato Dextrose Agar (PDA) were used for the enumeration of total heterotrophic bacteria and fungi respectively. Soil CO2-evolution was estimated every 5-days for 25 days. Total nitrogen, available phosphorus, dehydrogenase activity, Chemical Oxygen Demand (COD), Biochemical Oxygen Demand (BOD) and Dissolved Oxygen (DO) were also determined . Bacillus subtillis, Bacillus macerans, Pseudomonas aeruginosa, Psedomonas putida and A. niger were of common occurrence in all soil samples. The total bacterial counts in the farmland soils which had received pesticide treatment in Egbe (9.330 × 105 ±0.278 CFU/g), Ijele (10.170 ×105±0.211 CFU/g) and imaka(9.47 × 105 ±0.334 CFU/g) were higher than control (7.100 ×105 ±0.177 CFU/g, 7.470 ×105 ±0.186 CFU/g, 6.72 ×105 ±0.125 CFU/g) soil samples respectively. The total fungal counts (1.130 ×105±0.126 CFU/g,0.850 ×105±0.050 CFU/g, 0.680 ×105±0.048 CFU/g, 1.10 ×105±0.037 CFU/g) at the point of pollution at Egbe, Ibido, Ijele and Imaka respectively were found to be higher than their respective control soil samples. The BOD ranged from 15.837±0.187 to 20.853±0.254 mg/L. The DO, COD and BOD of the control water samples were significantly (P≤0.05) higher than the values obtained at the point of pollution. This study indicated the extent of microbial and pesticide pollution; further addition of wastes may deteriorate the existing hygienic quality of water in these locations.
Keywords: BOD, COD, DO, Total Nitrogen

1. INTRODUCTION

The use of pesticides in agricultural production whilst maintaining water quality is a major challenge in Nigeria. This has become increasingly significant as a result of the role of pesticides for effective production of food crops and industrial raw materials. Pesticides are used to control insects, weeds, and plant diseases which have negative impact on maximum plant growth, development, yields and marketability of crops, thereby ensuring sustainability of food production and availability of food all year

round (Lugushie and Atabila, 2012). When pesticides are applied on farmlands it can result in the pollution of water bodies by surface runoff, leaching (matrix flow) and preferential flow. Movement of pesticides from soil to water depends on factors such as soil texture, soil organic matter (FAO, 1996; Pierzynski et al., 2000; Filizola et al., 2002; Beitz et al., 1994), topography and rainfall (De Rossi et al., 2003; Tang et al., 2012). Pesticides which are highly adsorbed by soil mineral and organic particles have a lower leaching potential and consequently a high potential for being transported by surface runoff along with the sediments (Cheah et al., 1997).

Accumulation of such toxic water basically into the soil and water ultimately enter the food chain and cause health hazards. These toxic substances are either organic or inorganic compounds (Maibam et al., 2014). A number of quality parameters such as pH, color, turbidity, suspended solids, temperature, conductivity, odor, COD, BOD, DO, total nitrogen, total phosphate, total pesticides and Biological properties such as total faecal coliform counts, faecal streptococci counts, Salmonella counts are measured to determine water quality (Maibam et al., 2014).

The developed countries suffer from problems of chemical discharge into the water sources mainly groundwater, while developing countries face problems of agricultural run-off in water sources. Some studies reported the presence of pesticides in the surface water close to agriculture lands (Oudney et al., 2009; Anasco et al., 2010). Pesticides can get into water through drift during pesticides spraying, by runoff from treated area and leaching via the soil. This study determined microbial activities and physicochemical properties of pesticide treated soils and waters.

2. MATERIALS AND METHODS

Characteristics of Areas Where the Rivers are Located

This study was carried out in Odogbolu Local Government Area (Latitude 6.78597 and longitude 3.80511) South Western Nigeria (Figure, 1). The farm lands are located in Egbe (Latitude 6.75, Longitude 3.9528), Ijele (Latitude 6.74, Longitude 3.810739), Ibido (Latitude 6.75, Longitude 3.91667) and Imaka (Latitude 6.75, Longitude 3.9528) all in the same local government area (Figure 1). Each of the farm lands (all the rivers have farmlands that use both insecticides and herbicides close to their banks) were situated close to the bank of rivers. The rivers are used for several activities such as washing, bathing and drinking. Odogbolu has a tropical climate. The summers are much rainier than the winters in Odogbolu. The Köppen-Geiger climate classification is Aw. The temperature here averages 27.2^{o}C. The rainfall in Odogbolu averages 1539 mm. The driest month is December, with 14 mm of rainfall. The greatest amount of precipitation occurs in June, with an average of 274 mm. The warmest month of the year is March with an average temperature of 29.0 ^{o}C. The lowest average temperatures in the year occur in August, when it is around 25.3 ^{o}C.

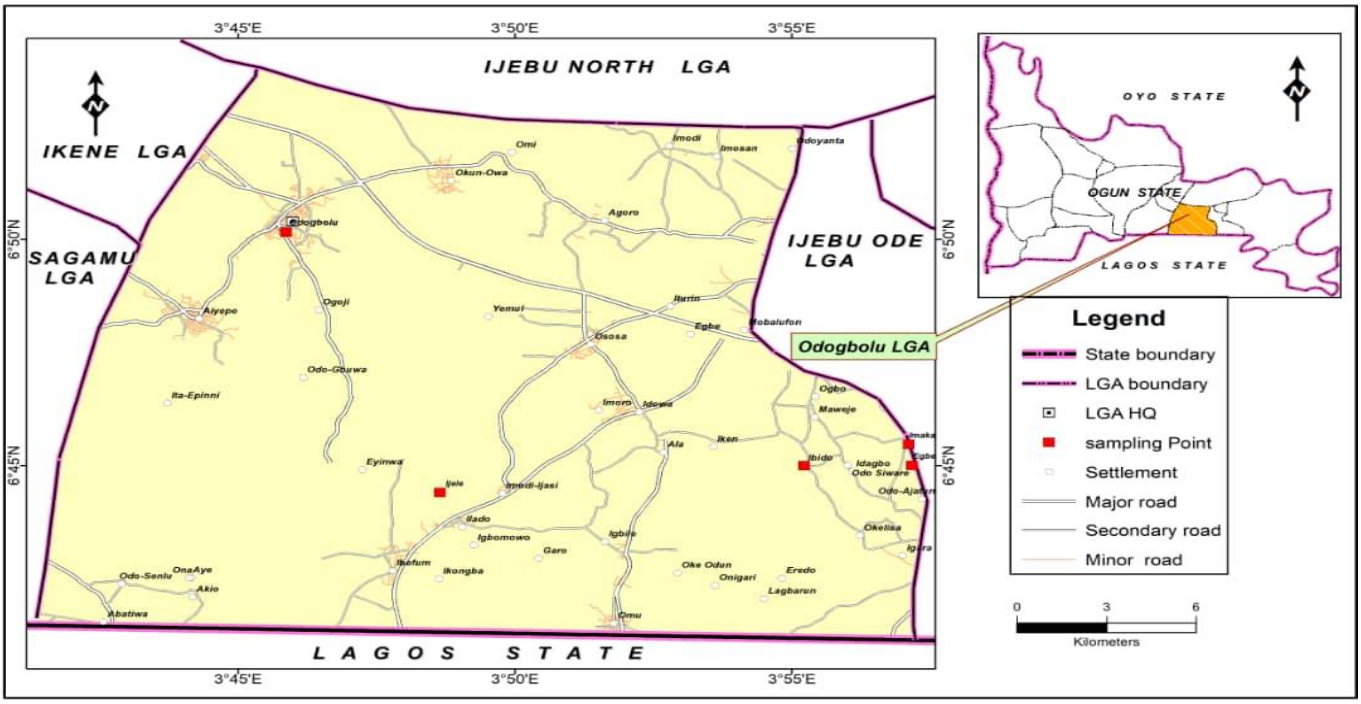

Figure 1. A map showing the longitude and latitude of pollution points.

Pesticides Used on The Farmlands

A survey of the most applied pesticides in the region was carried out. As a result, insecticide such as: Bentaforce (Bentzone sodium Salt, 40% SL Bentazothiadiazine), and herbicides which include; Weed cut (Paraquat Dichloride- 276 g/L), Atraforce (Atrazine 80% wp, 270 g/L) and Force up (Glyphosate-Isopropylamine Salt, 360 g/L) which were discovered to be commonly used in the farmlands close to the rivers were chosen for analysis in the present study.

Microbial Isolation, Enumeration and Identification

Nutrient agar (NA) was used for the enumeration of total heterotrophic bacteria by the pour plate method. Incubation was done at 30^0C for 24-48 h. Enumeration and isolation of fungi was carried out using Potato Dextrose Agar (PDA) and incubated at 25^oC for 7days. Bacterial isolates were characterized based on cultural characteristics, staining reactions and biochemical reactions. Identification was thereafter made with reference to Bergey's Manual of Systemic Bacteriology (1984). Morphological and cultural characteristics were used for fungi identification. The bacteria and fungi that emerged from plates were sub-cultured repeatedly until pure cultures were obtained. Counts of microorganisms were taken from plates containing 15-150 colonies per plates using the Quebec colony counter and this was used to calculate the number of colony forming units per gram (cfu/g) in each soil sample.

Microbial Respiration

Microbial respiration was carried out using the method of Klimek (2012). One hundred grams treated and untreated soil samples were placed in 1000 mL wide neck screw top glass jars containing 10mL of NaOH 0.1N solution in separate vials. Soil samples were incubated in the dark at 25oC+ 0.5. Soil moisture content was maintained at 60% water holding capacity by weighing and correcting for any weight loss, using sterile ultra pure water. Soil CO2-evolution was regularly (5-days interval period) estimated

during the twenty-five days incubation period. CO2 recovered in each NaOH solution was measured by titration with HCl, following the addition of BaCl2. Percentage CO2 evolved was then calculated.

Determination of Total Nitrogen

Ten grams of soil was weighed into 250 ml bottle and 100ml of 2M KCl was added, the bottle was stoppered and shaken on a mechanical shaker for 1 hour. The suspension was then filtered through whatman No. 42 filter paper and an aliquot for the analysis of the nitrogen form required was taken and refrigerated. Available nitrogen (NH_4-N and NO_3-N) in soil samples were then determined using the method of Landon (1984, 1991). Total nitrogen in soil samples was determined using macro-Kjeldhal distillation method. The nitrogen in the distillate was then determined by titration (Page et al., 1982).

Determination of Available Phosphorus in Soil

Five grams of air-dried soil sample (passed through 2mm sieve) was weighed into centrifuge tube and 20ml of extracting solution added. The mixture was then shaken for 1 minute on a mechanical shaker and centrifuged at 2000rpm for 15 minutes. Two millilitres of clear supernatant was then dispensed into 20ml test tube with a pipette. Five millilitres of distilled water and 2ml of ammonium molybdate solution was then added. The content was then mixed properly and 1ml of $SnCl_2.2H_2O$ dilute solution was then added and mixed again. After 5 minutes % transmittance was measured on spectronic-20 electrophotometer at 660nm wave length. Standard curve within the range of 0.1µgP/mL (ppm P) was then prepared. optical density of the standard solution was plotted against the ppm P and the content of the extractable P in the soil was calculated.

Determination of Dehydrogenase Activity

6g of soil and 6 ml of water samples were dispensed separately into 500ml conical flasks. 30ml glucose, 1ml of 2,3,5-triphenyl tetrazolium chloride (TTC) solution plus 2.5ml of distilled water were added and shaken on a shaker for 5min. The mixtures were then filtered through a double layered filter paper into 250ml conical flask having formed 1,3,5-triphenyl formazan (TPF). A stock solution of 0.2µmol/mL of TPF was prepared by dissolving 0.03g TPF in 500ml methanol. Working standard solutions of range 0.004 – 0.10 µmol/mL TPF were prepared from the stock solution to get the gradient factor. The absorbances of sample extract above and that of different working standard solutions were read on a UV/V Cecil Spectrophotometer at a wavelength of 485nm.

Determination of Dissolved Oxygen (DO)

Dissolved Oxygen was determined using the method of APHA (1998). This was done using Winkler's method. In this procedure, an excess of Manganese (II) salt, iodide (I-) and hydroxide (OH-) ions were added to the samples causing a white precipitate of Mn(OH)2 to form. This precipitate was then oxidized by the dissolved oxygen in the water sample into a brown Manganese precipitate. In the next step, a strong acid (either hydrochloric acid or sulphuric acid) was added to acidify the solution. The brown precipitate then converted the iodide ion (I-) to iodine. The amount of DO was directly proportional to the titration of iodine with a thiosulphate solution. In this study, 300ml BOD bottles were filled with the samples respectively, 2ml of manganese sulphate and 2ml of alkali-iodide-azide solution added by inserting a pipette just below the surface of the liquid. The bottles were stoppered to avoid the introduction of air and were mixed by inverting several times. The bottles were left to stand for a few minutes. The presence of oxygen was indicated by the formation of a brownish orange precipitate. Two millimeters (2ml) of H2SO4 was added to the samples. It was mixed again by inverting to dissolve the precipitate. Two hundred and one

milliliter of the sample was then measured into a clean 250ml conical flask and titrated against sodium thiosulphate Solution (Na2S2O35H2O) using the starch indicator until the solution turned colorless.

Calculation:

DO (mg/L) = [16000 x M xV] / [$V_2/V_1(_{V1-2})$]
Where = Molarity of thiosulpahte used.
V = volume of thiosulphate used for titration
V1 =Volume of bottle with stopper
V2 = Volume of aliquot taken for titration.

Chemical Oxygen Demand (COD)

Determination of COD was carried out according to the method described by Ademoroti (1996). 0.4 g HgSO4, 20 ml of water sample, 2 ml sulphuric acid and 10 ml of standard K2Cr2O7 solution and some glass beads was placed into a reflux with gentle swirling, 30 ml of Ag2SO reagent was slowly added, and refluxed for about two hours and cooled. The condenser was then washed with distilled water into Erlenmeyer flask and diluted to 150 ml with distilled water. The solution was allowed to cool to room temperature. The solution was then titrated with standard ferrous ammonium sulphate (FAS) using ferroin indicator.

The blank titration was carried out as above but using distilled water in place of the sample. The COD of the water sample was calculated from the following expression.

$$\text{COD (mg/L)} = \frac{(Vb - Vs) \times M \times 16000}{\text{ml of sample}}$$

where Vb = Volume of FAS for Blank;
Vs = Volume of FAS for sample;
M = Molarity of FAS.

Determination of Biochemical Oxygen Demand (BOD)

The method involves filling the samples to overflowing, in an airtight bottle of the specified size and incubating it at the specified temperature for 5days. DO was measured initially and after incubation and the BOD was computed from the difference between initial and final DO. Because the initial DO was determined shortly after the dilutions was added, all oxygen uptake occurring after this measurement was included in the BOD measurement. One Millimeter (1ml) of MgSO4, CaCl2, phosphate buffer, FeCl3 were added to 1L of water. The solution was then shaken thoroughly to saturate the dissolved oxygen. This solution was used to dilute samples. One hundred millimeters (100ml) of the samples were measured into different one Liter flasks and were made up to (1L) mark with the dilution water previously prepared. The dilution sample solution was then dispensed into BOD bottles and subsequently incubated at 20oC in the dark for 5 days (APHA, 1998).

$$BOD5 = DOi - DOf$$

Or

$$\frac{(Doi - Dof) \times \text{vol of BOD bottle}}{\text{vol of water sample}}$$

Statistical Analysis

Pearson's correlation coefficient between the measured variables was determined. Pearson's correlation coefficients were calculated at $P \leq 0.01$ and $P \leq 0.05$. The data were statistically analysed, with SPSS version 20 software, using a one-way analysis of variance (ANOVA).

3. RESULTS

Presented in Table 1, are bacteria and fungi isolated from the soil samples obtained from the various farmlands. *Bacillus subtillis, Bacillus macerans, Pseudomonas aeruginosa,* and *Pseudomonas putida* were prevalent in all the soil samples analyzed. *Aspergillus* species were isolated in all the soils analyzed. *Aspergillus niger* was isolated in all soil samples analyzed except Ijele, Imaka and Ibido points of pollution (Table 2).

Table 1. Bacteria and fungi isolated from soil samples in selected locations

SOIL SAMPLE	**BACTERIA**
Ibido Control	*B. cereus, B. macerans, B. subtilis, P. aureginosa, S. marscences P. putida, S. aureus, S. faccium,*
Ibido POPL	*P. putrefaciens, B. linchinefomis, B. macerans, B. subtilis, B. cereus, M. acidiophilus, M. luteus, P. putida, S. aureus*
Imaka Control	*B. subtilis, B. macerans, Micro. acidiophilus, P. aureginosa, P. vulgaricus, S. aureus*
Imaka POPL	*B. cereus, B. macerans, B. putrefaciens,P. florescences, P. mirabilis, P. vulgaricus, S. faecalis,*
Egbe Control	*Aerobacter aerogenes, B. subtilis, M. acidiophilus, M. luteus, P. aureginosa, P. putida,*
Egbe POPL	*Aerobacter aerogenes, B. macerans, B. subtilis, Clostridium sp, P. aureginosa, P. florenscences, P. putida, S. lactis,*
Ijele Control	*B. macerans, B. subtilis, M. luteus, P. aureginosa, P. vulgaricus, S. aureus, S. lactis,*
SOIL SAMPLE	**FUNGI**
Ibido Control	*A. niger, P. oxalicum, F. oxysporum .*
Ibido POPL	*A. tamarii, F. compacticum, F. oxysporum,*
Imaka Control	*A. niger, F. compacticum, F. oxysporum, P. oxalicum.*
Imaka POPL	*A. tamarii, A. tereus, F. oxysporum, P. chrysogenum, P. oxalicum.*
Egbe Control	*A. niger, A. tamarii, A. tereus, F. compacticum, P. citrinium, P. oxalicum*
Egbe POPL	*A. niger, A. fumigatus, A. flavus, A. terreus, F. equsetti, P. oxalicum*
Ijele Control	*A. niger, A. tamarii, F. oxysporum, P.oxalicum.*
Ijele POPL	*A. fumigatus, A. tamarii, A. tereus, F. oxysporum, P. chrysogenum, P. oxalicum.*

POPL= Point of pollution

Figure 2a, 2b, 2c, 2d shows the picture of the Egbe, Ibido, Ijele and imaka rivers. The Egbe River is used for several activities such as fishing, washing of clothes, bathing and drinking. There have also been reports of the presence of Alligator Crocodiles in this river. The rivers are constantly polluted with human faeces and urine.

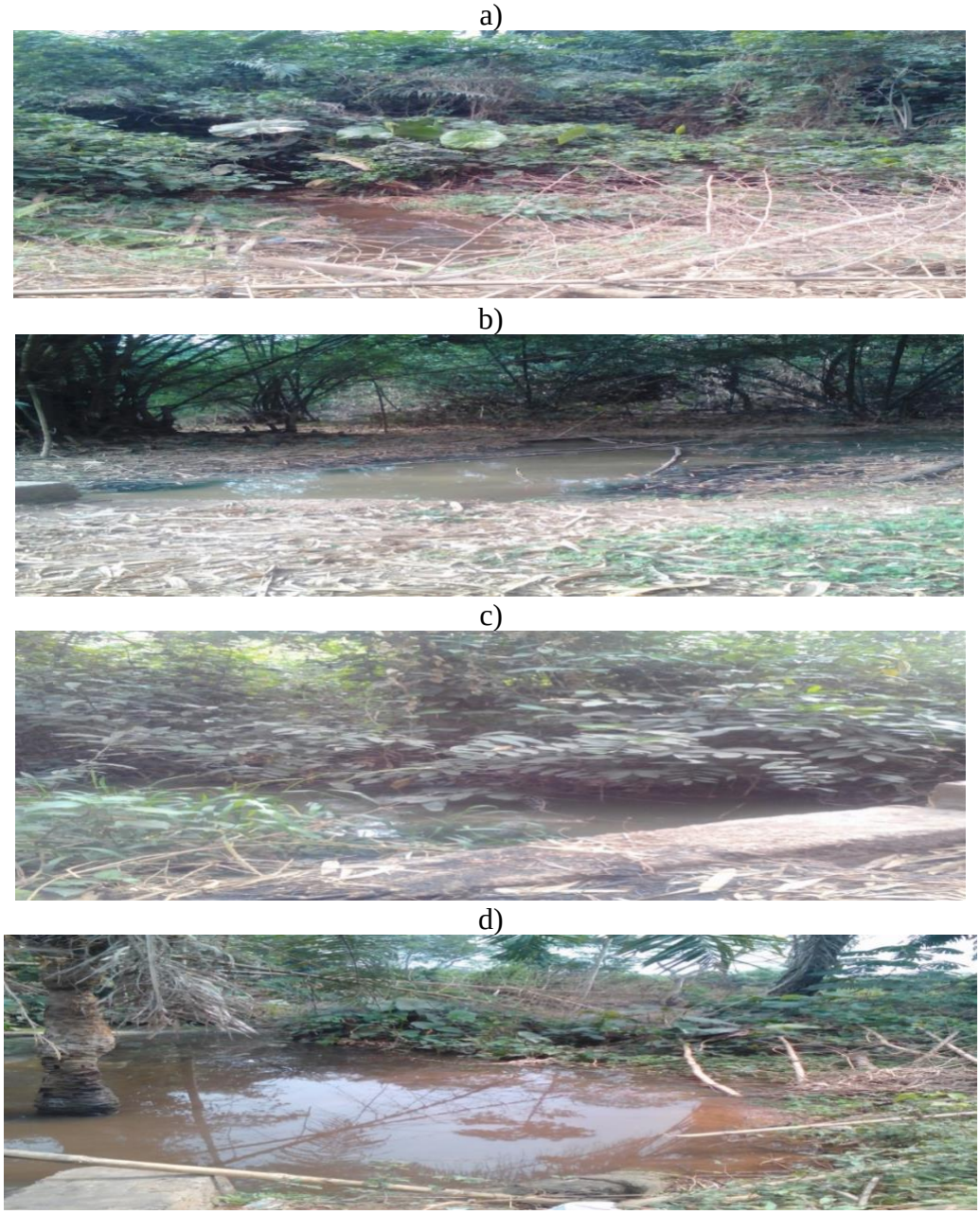

Figure 2. Photographs showing rivers used in this study (a) Egbe river (b) Ibido river (c) Ijele river (d) Imaka river.

In Table 2a, there were significant changes ($P \leq 0.05$) in the microbial counts, microbial activity (microbial respiration and dehydrogenase activity), available phosphorus, total nitrogen and pesticide concentration of the polluted soil samples in all the locations analyzed. The total bacterial counts in the farmland soils which had received pesticide treatment in Egbe ($9.330 \times 10^5 \pm 0.278$ CFU/g), Ijele ($10.170 \times 10^5 \pm 0.211$ CFU/g) and imaka($9.47 \times 10^5 \pm 0.334$ CFU/g) were higher than control ($7.100 \times 10^5 \pm 0.177$ CFU/g, $7.470 \times 10^5 \pm 0.186$ CFU/g, $6.72 \times 10^5 \pm 0.125$ CFU/g) soil samples respectively. In Ibido farmland the total bacterial count ($8.150 \times 10^5 \pm 0.326$ CFU/g) in the pesticide treated soils was lower than that obtained in the control soil samples ($11.100 \times 10^5 \pm 0.313$ CFU/g). The total coliform count in the pesticide treated soils of Ibido ($5.470 \times 10^5 \pm 0.109$ CFU/g), Ijele ($6.030 \times 10^5 \pm 0.095$ CFU/g) and Imaka ($6.58 \times 10^5 \pm 0.070$ CFU/g) were found to be higher than their control soil samples ($4.320 \times 10^5 \pm 0.117$, $5.400 \times 10^5 \pm 0.052$, 4.05 ± 0.120 CFU/g) respectively. Meanwhile in the Egbe farmlands the total coliform count in the control ($5.450 \times 10^5 \pm 0.056$ CFU/g) soil samples was higher than that of the pesticide treated soils (4.400

$\times 10^5 \pm 0.291$ CFU/g). The total fungal counts ($1.130 \times 10^5 \pm 0.126$ CFU/g,$0.850 \times 10^5 \pm 0.050$ CFU/g, $0.680 \times 10^5 \pm 0.048$ CFU/g, $1.10 \times 10^5 \pm 0.037$ CFU/g) at the point of pollution at Egbe, Ibido, Ijele and Imaka respectively were found to be higher than their respective control soil samples. Soils that have received pesticide treatment showed higher microbial counts except the total coliform count (Egbe) and total bacterial count (Ibido). Microbial respiration (1.470 ± 0.029 $\mu g g^{-1}$, 1.190 ± 0.007 $\mu g g^{-1}$, 1.300 ± 0.010 $\mu g g^{-1}$, 1.29 ± 0.007 $\mu g g^{-1}$) in soils that received pesticide treatment in Egbe, Ibido, Ijele and Imaka respectively were higher than their respective control soil samples (0.600 ± 0.009 $\mu g g^{-1}$, 1.050 ± 0.022 $\mu g g^{-1}$, 0.820 ± 0.026 $\mu g g^{-1}$, 0.63 ± 0.042 $\mu g g^{-1}$). The available phosphorus, dehydrogenase activities and total nitrogen content of soil samples at the point of pollution, in all the farmlands analyzed in this study, were higher than their control soil samples. All the farmland soils analyzed in this study showed the presence of the three herbicides (Weed cut, Atraforce, Force up) and insecticide (Bentaforce). The herbicide Force up had the highest concentration (0.089 ± 0.001 $\mu g\ g^{-1}$) at Imaka farmland.

Presented in Table 2b are the microbial counts, microbial activity (microbial respiration and dehydrogenase activity), available phosphorus, total nitrogen, dissolved oxygen, biochemical oxygen demand and chemical oxygen demand of water polluted with pesticides. There were significant changes in all the variables analyzed in Table 2. The total bacterial counts and the total fungal counts of the control water samples obtained from Egbe, Ijele, Ibido and Imaka were found to be lower than the counts obtained at the point of pollution. The highest total bacterial count of $9.933 \times 10^5 \pm 0.305$ CFU/g was obtained in polluted water obtained at Imaka, while the highest fungal count of $0.567 \times 10^5 \pm 0.042$ CFU/g was obtained at the Ijele polluted water samples. The total coliform count of the control water samples obtained at Ibido, Ijele and Imaka were found to be higher than the values obtained at the point of pollution. Meanwhile the total coliform count of the control water samples obtained at Egbe were found to be lower than the total coliform count obtained at the point of pollution. The highest coliform count of $6.733 \times 10^5 \pm 0.235$ CFU/g was obtained in the water samples obtained at the point of pollution in Egbe. Microbial respiration, dehydrogenase activities and total nitrogen were found to be highest at the point of pollution of the water samples compared to the control. The highest microbial respiration, dehydrogenase activity and total nitrogen values of 0.165 ± 0.002 $\mu g g^{-1}$, 0.012 ± 0.000 $\mu g g^{-1}$ and 0.017 ± 0.001 % respectively were obtained at the point of pollution in Ijele. Available phosphorus was found to be highest at the point of pollution of the water samples compared to the control. The highest available phosphorus value of 7.767 ± 0.056 % was obtained at the point of water pollution at Imaka. The dissolved oxygen, chemical oxygen demand and the biochemical oxygen demand of the control water samples were significantly ($P \leq 0.05$) higher than the values obtained at the point of pollution. The highest dissolved oxygen value of 6.183 ± 0.031 mg l^{-1} was obtained in the control water samples of Imaka. Meanwhile the highest biochemical oxygen demand value of 20.853 ± 0.254 mg l^{-1} was obtained in the control water samples of Egbe. The BOD ranges from 15.837 ± 0.187 to 20.853 ± 0.254 mg/L.

Table 2a. Microbial counts, microbial activity (microbial respiration and dehydrogenase activity), available phosphorus, total nitrogen and pesticide concentration in polluted soils.

		EGBE	IBIDO	IJELE	IMAKA
TBC ($\times 10^5$ CFU/g)	CONT	7.100±0.177	11.100±0.313	7.470±0.186	6.72±0.125
	POPL	9.330±0.278	8.150±0.326	10.170±0.211	9.47±0.334
TCC($\times 10^5$CFU /g)	CONT	5.450±0.056	4.320±0.117	5.400±0.052	4.05±0.120
	POPL	4.400±0.291	5.470±0.109	6.030±0.095	6.58±0.070
TFC($\times 10^5$CFU /g)	CONT	0.350±0.050	0.470±0.042	0.370±0.021	0.55±0.050
	POPL	1.130±0.126	0.850±0.050	0.680±0.048	1.10±0.037
MR ($\mu g g^{-1}$)	CONT	0.600±0.009	1.050±0.022	0.820±0.026	0.63±0.042
	POPL	1.470±0.029	1.190±0.007	1.300±0.010	1.29±0.007
AP($mgkg^{-1}$)	CONT	6.420±0.100	6.540±0.031	5.680±0.107	6.35±0.019

	POPL	8.790±0.054	7.800±0.196	7.890±0.342	8.61±0.023
DEH(μgg^{-1})	CONT	0.010±0.001	0.010±0.000	0.010±0.001	0.01±0.001
	POPL	0.030±0.002	0.020±0.002	0.040±0.001	0.03±0.001
TN (%)	CONT	0.050±0.002	0.050±0.002	0.050±0.001	0.04±0.001
	POPL	0.080±0.001	0.080±0.001	0.070±0.003	0.07±0.002
BF(μg g^{-1})	CONT	0.001±0.000	0.002±0.000	0.002±0.000	0.001±0.000
	POPL	0.018±0.001	0.034±0.015	0.022±0.001	0.012±0.001
WC(μg g^{-1})	CONT	0.002±0.000	0.001±0.000	0.001±0.000	0.001±0.000
	POPL	0.038±0.001	0.057±0.002	0.057±0.001	0.042±0.001
AF(μg g^{-1})	CONT	0.001±0.000	0.001±0.000	0.001±0.000	0.001±0.000
	POPL	0.025±0.001	0.020±0.001	0.053±0.001	0.035±0.002
FU(μg g^{-1})	CONT	0.001±0.000	0.001±0.000	0.001±0.000	0.001±0.000
	POPL	0.074±0.001	0.075±0.002	0.066±0.001	0.089±0.001

TBC= Total Bacterial Count, TCC= Total Coliform Count, TFC= Total Fungal count MR= Microbial respiration, AP = Available Phosphorus, DEH= Dehydrogenase Activity, TN= Total Nitrogen, BF= Benta Force, WC= Weed Cut, AF= Atra Force, FU= Force Up, CONT = Control, POPL= Point of Pollution

Table 2b. Microbial counts, microbial activity and physicochemical parameters of water polluted with pesticides

		EGBE	IBIDO	IJELE	IMAKA
TBC	CONT	4.617±0.048	5.350±0.123	4.900±0.277	4.933±0.292
(×10^{5}CFU/g)	POPL	8.667±0.099	7.850±0.214	8.517±0.335	9.933±0.305
TCC	CONT	3.783±0.105	4.050±0.120	4.667±0.112	3.600±0.058
(×10^{5}CFU/g)	POPL	6.733±0.235	1.367±0.096	1.450±0.062	1.717±0.040
TFC	CONT	0.233±0.021	0.233±0.021	0.233±0.021	0.233±0.021
(×10^{5}CFU/g)	POPL	0.533±0.042	0.500±0.045	0.567±0.042	0.467±0.042
MR(μgg^{-1})	CONT	0.007±0.000	0.109±0.001	0.005±0.000	0.039±0.020
	POPL	0.154±0.001	0.129±0.003	0.165±0.002	0.144±0.001
AP(mgkg^{-1})	CONT	5.700±0.037	5.810±0.026	5.433±0.173	5.287±0.105
	POPL	7.547±0.193	6.875±0.022	7.600±0.228	7.767±0.056
DEH(μgg^{-1})	CONT	0.003±0.000	0.003±0.000	0.003±0.000	0.003±0.000
	POPL	0.010±0.001	0.005±0.000	0.012±0.000	0.008±0.001
TN(%)	CONT	0.003±0.000	0.004±0.000	0.003±0.000	0.003±0.000
	POPL	0.012±0.001	0.007±0.000	0.017±0.001	0.010±0.001
DO(mg l^{-1})	CONT	6.848±0.132	7.237±0.107	6.877±0.023	6.970±0.030
	POPL	5.690±0.038	6.033±0.080	5.578±0.058	6.183±0.031
BOD(mg l^{-1})	CONT	20.853±0.254	19.267±0.377	19.150±0.316	20.567±0.362
	POPL	16.270±0.115	15.837±0.187	16.117±0.128	16.150±0.188
COD(mg l^{-1})	CONT	39.833±0.470	40.217±0.554	41.567±0.451	40.440±0.350
	POP	28.100±0.241	26.033±0.401	26.300±0.260	28.950±0.433

TBC= Total Bacterial Count, TCC= Total Coliform Count, TFC= Total Fungal count MR= Microbial respiration, AP= Available Phosphorus, DEH= Dehydrogenase Activity, TN= Total Nitrogen, DO= Dissolved Oxygen, BOD= Biochemical Oxygen Demand, COD= Chemical Oxygen Demand. CONT= Control, POPL= Point of pollution.

In Tables 3a, 3b, 3c and 3d, Dissolved oxygen, biochemical oxygen demand and chemical oxygen demand showed strong negative correlations with total bacterial count and total fungal count in all locations

examined. The strongest correlation of dissolved oxygen with total bacterial (r=-0.936; P≤0.01) count and total fungal count (r=-0.827; P≤0.01) occurred in Imaka water samples, while the strongest correlation of biochemical oxygen demand with total bacterial (r=--0.988; P≤0.01) count and total fungal count (r=-0.914; P≤0.01) occurred in Egbe water samples.

Table 3a. Correlations of selected variables in Ibido water sample

	DO	BOD	COD	TBC	TCC	TFC	MR	AP	DEH	TN
DO		0.774**	0.916**	-0.908**	0.958**	-0.736**	-0.818**	-0.930**	-0.799**	-0.881**
BOD	0.774**		0.950**	-0.903**	0.892**	-0.878**	-0.886**	-0.928**	-0.970**	-0.919**
COD	0.916**	0.950**		-0.945**	0.963**	-0.815**	-0.938**	-0.973**	-0.963**	-0.967**
TBC	-0.908**	-0.903**	-0.945**		-0.931**	0.819**	0.875**	0.945**	0.882**	0.950**
TCC	0.958**	0.892**	0.963**	-0.931**		-0.845**	-0.837**	-0.976**	-0.882**	-0.892**
TFC	-0.736**	-0.878**	-0.815**	0.819**	-0.845**		0.721**	0.893**	0.839**	0.752**
MR	-0.818**	-0.886**	-0.938**	0.875**	-0.837**	0.721**		0.895**	0.958**	0.960**
AP	-0.930**	-0.928**	-0.973**	0.945**	-0.976**	0.893**	0.895**		0.939**	0.929**
DEH	-0.799**	-0.970**	-0.963**	0.882**	-0.882**	0.839**	0.958**	0.939**		0.943**
TN	-0.881**	-0.919**	-0.967**	0.950**	-0.892**	0.752**	0.960**	0.929**	0.943**	

TBC= Total Bacterial Count, TCC= Total Coliform Count, TFC= Total Fungal count MR= Microbial respiration, AP= Available Phosphorus, DEH= Dehydrogenase Activity, TN= Total Nitrogen, DO= Dissolved Oxygen, BOD= Biochemical Oxygen Demand, COD= Chemical Oxygen Demand. **Correlation is significant at the 0.01 level (2-tailed), *Correlation is significant at the 0.05 level (2-tailed).

Table 3b. Correlations of selected variables in Egbe water sample

	DO	BOD	COD	TBC	TCC	TFC	MR	AP	DEH	TN
DO		0.862**	0.897**	-0.916**	-0.913**	-0.756**	-0.938**	-0.926**	-0.764**	-0.832**
BOD	0.862**		0.977**	-0.988**	-0.956**	-0.914**	-0.981**	-0.906**	-0.918**	-0.937**
COD	0.897**	0.977**		-0.991**	-0.927**	-0.926**	-0.989**	-0.941**	-0.901**	-0.933**
TBC	-0.916**	-0.988**	-0.991**		0.959**	0.925**	0.996**	0.927**	0.921**	0.948**
TCC	-0.913**	-0.956**	-0.927**	0.959**		0.810**	0.962**	0.867**	0.843**	0.859**
TFC	-0.756**	-0.914**	-0.926**	0.925**	0.810**		0.894**	0.787**	0.980**	0.975**
MR	-0.938**	-0.981**	-0.989**	0.996**	0.962**	0.894**		0.952**	0.890**	0.928**
AP	-0.926**	-0.906**	-0.941**	0.927**	0.867**	0.787**	0.952**		0.757**	0.843**
DEH	-0.764**	-0.918**	-0.901**	0.921**	0.843**	0.980**	0.890**	0.757**		0.980**
TN	-0.832**	-0.937**	-0.933**	0.948**	0.859**	0.975**	0.928**	0.843**	0.980**	

TBC= Total Bacterial Count, TCC= Total Coliform Count, TFC= Total Fungal count MR= Microbial respiration, AP= Available Phosphorus, DEH= Dehydrogenase Activity, TN= Total Nitrogen, DO= Dissolved Oxygen, BOD= Biochemical Oxygen Demand, COD= Chemical Oxygen Demand. **Correlation is significant at the 0.01 level (2-tailed), *Correlation is significant at the 0.05 level (2-tailed).

Table 3c. Correlations of selected variables in Ijele water sample

	DO	BOD	COD	TBC	TCC	TFC	MR	AP	DEH	TN
DO		0.925**	0.982**	-0.895**	0.981**	-0.859**	-0.984**	-0.859**	-0.983**	-0.954**
BOD	0.925**		0.956**	-0.861**	0.942**	-0.897**	-0.944**	-0.839**	-0.972**	-0.932**
COD	0.982**	0.956**		-0.905**	0.998**	-0.898**	-0.995**	-0.908**	-0.994**	-0.986**
TBC	-0.895**	-0.861**	-0.905**		-0.899**	0.972**	0.929**	0.955**	0.887**	0.934**
TCC	0.981**	0.942**	0.998**	-0.899**		-0.884**	-0.993**	-0.908**	-0.988**	-0.986**
TFC	-0.859**	-0.897**	-0.898**	0.972**	-0.884**		0.913**	0.945**	0.885**	0.931**
MR	-0.984**	-0.944**	-0.995**	0.929**	-0.993**	0.913**		0.929**	0.989**	0.991**
AP	-0.859**	-0.839**	-0.908**	0.955**	-0.908**	0.945**	0.929**		0.876**	0.959**
DEH	-0.983**	-0.972**	-0.994**	0.887**	-0.988**	0.885**	0.989**	0.876**		0.970**
TN	-0.954**	-0.932**	-0.986**	0.934**	-0.986**	0.931**	0.991**	0.959**	0.970**	

TBC= Total Bacterial Count, TCC= Total Coliform Count, TFC= Total Fungal count MR= Microbial respiration, AP= Available Phosphorus, DEH= Dehydrogenase Activity, TN= Total Nitrogen, DO= Dissolved Oxygen, BOD= Biochemical Oxygen Demand, COD= Chemical Oxygen Demand. **Correlation is significant at the 0.01 level (2-tailed), *Correlation is significant at the 0.05 level (2-tailed).

Table 3d. Correlations of selected variables in Imaka water sample

	DO	BOD	COD	TBC	TCC	TFC	MR	AP	DEH	TN
DO		0.957**	0.976**	-0.936**	0.981**	-0.827**	-0.798**	-0.960**	-0.819**	-0.919**
BOD	0.957**		0.972**	-0.962**	0.952**	-0.737**	-0.808**	-0.924**	-0.814**	-0.942**
COD	0.976**	0.972**		-0.975**	0.990**	-0.794**	-0.820**	-0.974**	-0.896**	-0.976**
TBC	-0.936**	-0.962**	-0.975**		-0.950**	0.712**	0.904**	0.967**	0.916**	0.972**
TCC	0.981**	0.952**	0.990**	-0.950**		-0.854**	-0.818**	-0.982**	-0.864**	-0.944**
TFC	-0.827**	-0.737**	-0.794**	0.712**	-0.854**		0.658*	0.822**	0.579*	0.670*
MR	-0.798**	-0.808**	-0.820**	0.904**	-0.818**	0.658*		0.898**	0.784**	0.795**
AP	-0.960**	-0.924**	-0.974**	0.967**	-0.982**	0.822**	0.898**		0.899**	0.939**
DEH	-0.819**	-0.814**	-0.896**	0.916**	-0.864**	0.579*	0.784**	0.899**		0.954**
TN	-0.919**	-0.942**	-0.976**	0.972**	-0.944**	0.670*	0.795**	0.939**	0.954**	

TBC= Total Bacterial Count, TCC= Total Coliform Count, TFC= Total Fungal count MR= Microbial respiration, AP= Available Phosphorus, DEH= Dehydrogenase Activity, TN= Total Nitrogen, DO= Dissolved Oxygen, BOD= Biochemical Oxygen Demand, COD= Chemical Oxygen Demand. **Correlation is significant at the 0.01 level (2-tailed).

4. DISCUSSION

DO levels less than 3 mg/L are stressful to most aquatic organisms. Most fish die at 1 - 2 mg/L. However, fish can move away from low DO areas. Water with low DO from 0.2 - 0.5 mg/L are considered hypoxic; waters with less than 0.5 mg/L are anoxic. The DO standard for sustaining aquatic life is stipulated at 5 mg/L a concentration below this value adversely affects aquatic biological life, while concentration below 2 mg/L may lead to death for most fishes (Chapman, 1993). The present findings reported DO values higher than 5 mg/L in all locations. Hence the DO values obtained in this study are found to be acceptable living conditions for living organisms in water. Hence the pollution of water samples in all the locations with pesticides did not cause significant stress to the aquatic life.

The BOD levels reported in this study were higher than the values reported as the standard EU guidelines of 3.0 to 6.0 mg/L . High BOD levels results in decrease of DO levels because the bacteria are making use of the limited oxygen that is available in water. Due to the low level of dissolved oxygen in water, fish and other aquatic organisms may not survive. The high BOD levels reported in this study is as a result of the several activities such as, defecating, washing, swimming etc. which occurs in the streams.

Similar results were reported by Akan et al. (2012), they stated that the BOD levels recorded in the entire sampling points, in their study, were higher than the EU guidelines of 3.0 to 6.0 mg/L.
In this study the least COD value of 26.033±0.401 mg/L was lower than the WHO limit of 200 mg/L. Conversely, Akan et al. (2012) reported that the least COD value detected at point S2 did exceed the WHO limit of 200 mg/L. The increasing trend in COD concentration in the five sampling point when compared to the WHO standard value is an indication of wastewater dis- charges from settlements along the Chari-Logone and Komadugu-Yobe River courses particularly from abattoirs, hotels and hospitals into the lake, and also from surface and ground flows that carry chemicals directly from agricultural field into the Lake (Keith and Plowes, 1997). The pesticide concentrations recovered from the pesticide treated farmland soils indicates the persistence of these pesticides in soils after use on crop plants (as insecticides) and in clearing weeds. However, pesticide concentrations in water samples were not reported because the concentrations obtained were negligible. This might have occurred as a result of biodegradation of the pesticides in water due to the presence of active pesticide degrading microbial populations.

The soils of the farm lands that had been treated with pesticide contained mainly Bacillus, Pseudomonas and Aspergillus species. These bacterial and fungal species have been reported to be good biodegraders of pesticides (Filimon et al., 2012). Increased microbial respiration, dehydrogenase activity, total nitrogen and available phosphorus observed in this study indicates increased microbial activity, which can in turn lead to increased biochemical oxygen demand in water samples. This is however dangerous to the health of living organisms in the aquatic environment. Similar to what was obtained in this study, high total coliform was also reported in the work of Badr et al. (2014). Mahesh and Prasanth (2015) reported that in their study, the range of total viable count (CFU/mL) and total coliform counts (CFU/mL) were in the range of 4.3 – 9.9 (x104) and 1.43 – 2.6 (x 103) respectively. They further reported that most of the sites were found to have high TVC in most of the water samples. Most of the samples were found to have TVC higher than suggested by the Bureau of Indian Standard limits (BIS, 1991). However, in this study the range of total viable counts and total coliform counts were higher than reported by Mahesh and Prasanth (2015). Heterotrophic bacteria commonly respond to pollution of this type by decomposing organic matter and releasing nutrients and energy (Obi et al., 2002). Constant visits to rivers by the populace and by livestock are common in developing countries. Especially, poor rural communities that have limited access to potable clean water and they largely reside near river banks (Mahesh and Prasanth, 2015). As a result, they often utilize river waters for their daily washings and defecation which results in pollution of these water bodies. These activities particularly deteriorate microbial water quality as fecal matter is disposed and the surrounding area is littered with feces.

5. CONCLUSION

This study has given indication of the extent of microbial and pesticide pollution; any further addition of wastes may deteriorate the existing hygienic quality of water in these locations. It is recommended that regular microbiological studies including supplemental bacterial indicators should form an integral part of coastal pollution monitoring programs.

6. REFERENCES

1. Akan, J.C., Abbagambo, M.T., Chellube, Z.M., Abdulrahman, F.I. (2012). Assessment of Pollutants in Water and Sediment Samples in Lake Chad, Baga, North Eastern Nigeria. *Journal of Environmental Protection*, 3, 1428-1441.

2. American Public Health Association (1998). *Standard Methods for the Examination of Water and Waste Water*, 20th Edition., Washington DC.

3. Badr, R., Holial, H., Olama, Z. (2014). Water quality assessment of hasbani river in south Lebanon: Microbiological and Chemical

Characteristics and their Impact on the *Ecosystem*. *Journal of Global Biosciences*, 3(2), 536-551.

4. Beitz, H., Schmidt, H., Herzel, F. (1994). Occurrence, toxicological and ecotoxicological significance of pesticides in groundwater and surface water. In: Börner H. Pesticides in ground and surface water. Springer-Verlag, Berlim.

5. Bureau of Indian Standard, Indian Standard (1991). Indian standards drinking water specification.

6. Chapman, D. (1993). Assessment of Injury to Fish Populations: Clark Fork River NPL Sites, Montana, In: J. Lipton, Ed., *Aquatic Resources Injury Assessment Report*, Upper Clark Fork Riverm Basin, Montana Natural Resource Damage Assessment Program, Helena, Mont, 1993.

7. Cheah, U.B., Kirkwood, R.C., Lum, K.Y. (1997). Adsorption, desorption and mobility of four commonly used pesticides in Malaysian agricultural soils. *Pesticide Science*, 50,53-63.

8. De Rossi, C., Bierl, R., Riefstah, J. (2003). Organic pollutants in precipitation: Monitoring of pesticides and polycyclic aromatic hydrocarbons in the region of Trier (Germany). *Physics and Chemistry of the Earth*, 28, 307–314.

9. Filimon, M.N., Popescu, R., Borozan, A.B., Bordean, D.M., Dumitrescu, G., Voia S.O. (2012). Influence of xenobiotic substances on actinomycete communities in soil. *Animal Science and Biotechnologies*, 45(2), 221-224.

10. Filizola, H.F., Ferracini, V.L., Sans, L.M.A., Gomes, M.A.F., Ferreira, C.J.A. (2002). Monitoring and evaluation of the risk of contamination by pesticide in surface water and groundwater in the Guaíra region, São Paulo, Brazil. *Brazilian Agricultural Research*, 37, 659-667.

11. Food Agriculture Organization of the United Nations (1996). Control of water pollution from agriculture. GEMS/Water Collaborating Centre-Canada Centre for Inland Waters, Burlington, Canada.

12. Keith, J. O., Plowes, D. C. H. (1997). Considerations of Wildlife Resources and Land Use in Chad," USAID Technical, Paper 47, 1997.

13. Klimek, B. (2012). Effect of Long-Term Zinc Pollution on Soil Microbial Community Resistance to Repeated Contamination. Bulletin of Environmental Contamination and Toxicology, 8(4), 617-622.

14. Lourençato, L.F., Favaretto, N., Hansel, F.A., Scheer, A., Junior, L.F.L., Souza, L.C., Dieckow, J., Buch, A.C. (2015). *International Journal of Plant & Soil Science*, 5(3), 155-166.

15. Lugushie, J.A., Atabila, A (2012). Effect of Organochlorine Pesticides Usage on Water Quality of Tano River in the Asunafo South District of Brong Ahafo Region of Ghana. *Advanced Research in Scientific Areas*, 3(7), 1357-1362.

16. Mahesh, V. and Prasanth, S. (2015). Occurrence of pollution indicators in tropical perennial river of Periyar, Southern India. International *Journal of Pharmacological Research*, 5(10), 264-268.

17. Nagvenkar, G.S., Ramaiah, N. (2009). Abundance of sewage-pollution indicator and human pathogenic bacteria in a tropical estuarine complex. *Environmental Monitoring Assessment*, 155,245–256.

18. Obi, C.L., Potgieter, N., Bessong, P.O. and Matsaung, G. (2002). Assessment of the microbial quality of river water sources in rural Venda communities in South Africa. *Water S.A.*, 28, 287–292.

19. Oudney, M.B., Ou, Z., Sekela, M., Tuominen, T., Gledhill, M. (2009):Pesticide Multiresidues in waters of the Lower Fraser Vally, British Columbia, Canada. Part1. Surface water. *Journal of Environmental Quality*, 38 (3), 940-947.

20. Page, A.L., Miller, R.H., Keeney (eds.) (1982). Methods of soil analysis: Part 2. Chemical and microbiological properties. 2nd ed. Agronomy Series 9, ASA, SSSA, Madison, Wis.

21. Pierzynski, G.M., Sims, J.T., Vance, G.F. (2000). Soils and environment quality. 2 ed. Boca Raton.

22. Tang, X., Zhu, B., Katou, H. (2012). A review of rapid transport of pesticides from sloping farmland to surface waters: Processes and mitigation strategies. *Journal of Environmental Sciences*, 24,351–361.

23. Vignesh, S., Muthukumar, K., Santhosh, G. M., Arthur, J. R. (2013). Microbial pollution indicators in Cauvery river, southern India. In Mu. Ramkumar (Ed.), On a Sustainable Future of the Earth's Natural Resources, Springer earth system sciences. 363–376

24. Williamson, S., Ball, A., Pretty, D. (2006) Trends in pesticides use and drivers for safer pest management in four African countries. *Crop Protection*, 27: 1327-1334.